

Titel:

Plaque deposition and microglia response under the influence of hypoxia in a murine model
of Alzheimer's disease

Dissertation
zur Erlangung des akademischen Grades
Dr. med.

an der Medizinischen Fakultät
der Universität Leipzig

eingereicht von: Adrian / Viehweger / 28.10.1986 / Meerane

angefertigt an / in:

1. Universidad de Sevilla / Instituto de Biomedicina de Sevilla (IBIS) / Hospital Virgen del Rocio / Sevilla
2. Universität Leipzig / Medizinische Fakultät / Universitätsklinikum / Leipzig

Betreuer:

1. Prof. J. López Barneo, M.D., Ph.D.
2. A. Pascual Bravo, Ph.D.
3. Prof. Dr. rer. nat. F. Gaunitz
4. Prof. Dr. med. J. Meixensberger

Beschluss über die Verleihung des Doktorgrades vom: 17.12.2013

List of contents

<i>Bibliography</i>	<i>i</i>
<i>List of abbreviations</i>	<i>ii</i>
<i>Introduction</i>	<i>1</i>
<i>1 Alzheimer's Disease</i>	<i>1</i>
<i>1.1 Clinical Appearance</i>	<i>1</i>
<i>1.2 Epidemiology</i>	<i>2</i>
<i>1.3 Pathophysiology</i>	<i>3</i>
<i>1.3.1 Genetic base</i>	<i>3</i>
<i>1.3.2 Protein base</i>	<i>4</i>
<i>1.3.3 Conclusion</i>	<i>5</i>
<i>2 From Risk Factors to Hypotheses</i>	<i>6</i>
<i>2.1 Non-Vascular Risk Factors</i>	<i>6</i>
<i>2.2 Vascular Risk Factors</i>	<i>7</i>
<i>3 Defining hypoxia</i>	<i>8</i>
<i>3.1 Oxygen sensing and signalling</i>	<i>8</i>
<i>3.2 Molecular findings linking HIF to AD</i>	<i>9</i>

4	<i>Microglia and AD</i>	10
4.1	<i>Origin, innate immunity, function, phenotype, activation</i>	10
4.2	<i>Microglia and hypoxia</i>	11

<i>Materials & Methods</i>	13
1 <i>Animals</i>	13
2 <i>Genotyping</i>	13
3 <i>Hypoxia treatments</i>	14
4 <i>Tissue preparation/ HCT measurement</i>	14
5 <i>Immunohistochemistry</i>	15
5.1 <i>Aβ1-42 staining</i>	15
5.2 <i>Iba1 staining</i>	16
6 <i>Other staining techniques</i>	16
6.1 <i>Thioflavin- S staining</i>	16
6.2 <i>Prussian staining</i>	17
6.3 <i>Hematoxylin and Eosin staining</i>	18
7 <i>Cell Culture</i>	18
8 <i>Immunocytochemistry</i>	19
9 <i>Hypoxia treatment of cells/ XTT assay</i>	20
10 <i>Protein extraction and quantification</i>	20
11 <i>Western blot (WB)</i>	21

12	<i>Dot blot</i>	22
13	<i>ELISA</i>	22
14	<i>Plaque load estimation/ Stereology/ Microglia count</i>	23
15	<i>Statistics</i>	25
16	<i>List of materials</i>	26

<i>Results</i>	30
1 <i>Working hypothesis</i>	30
2 <i>Physiologic response under the influence of hypoxia</i>	30
3 <i>Histology confirms the effect of the hypoxic treatment</i>	32
4 <i>Plaque load is not significantly affected by hypoxic treatment</i>	34
5 <i>Oligomer formation under hypoxic treatment</i>	38
6 <i>Microglia under hypoxic conditions</i>	39
7 <i>Correlation between the number of microglia and vessel density</i>	44
8 <i>Cultured microglial cells respond with increased viability to hypoxic stimuli</i>	45
9 <i>Plaque occupancy under hypoxia</i>	46

<i>Discussion</i>	48
1 <i>The hypothesis</i>	48
2 <i>The model</i>	49
3 <i>The variables</i>	50
4 <i>The results</i>	51
4.1 <i>Hypoxia induces response</i>	51
4.2 <i>Hypoxia and Aβ- quantity</i>	51
4.3 <i>Hypoxia and Aβ- quality</i>	54
4.4 <i>Hypoxia and microglia</i>	54
4.4.1 <i>Aβ- quantity is not altered by a decreased number of microglia</i>	58
4.4.2 <i>The number of microglia decreases under hypoxia</i>	61
4.5 <i>Summary</i>	64
5 <i>Future research</i>	64

Supplements

1. Summary
2. Literature
3. "Eigenständigkeitserklärung"
4. Curriculum vitae
5. Thanks to...

Bibliographische Beschreibung (Bibliography)

Viehweger, Adrian

Titel (Title):

Plaque deposition and microglia response under the influence of hypoxia in a murine model of Alzheimer's disease

Universität Leipzig, Dissertation

73 S., 139 Lit., 30 Abb., 3 Tab.

Referat (Abstract):

Clinical findings have linked multiple pathologies to Alzheimer's disease (AD), particularly associated with the vasculature. Coexistence worsens dementia, the clinical hallmark of the disease, as compared to pure AD. One general common denominator of these associated pathologies, such as stroke, is the presence of hypoxic tissue conditions. It was asked, whether there exists a mutual, causal interaction between hypoxia and AD pathology, that could explain the clinical observations. Alternatively, the worsened clinical state of multiple brain pathologies could "simply" be the consequence of multimorbidity, i.e. accumulated disease load, without any causal interaction between the constituents.

The experimental results from a murine model of AD demonstrate, that long-term exposure to hypoxia significantly reduces the number of microglia. Thus the microglia function to confront A β - protein plaques, a hallmark in AD pathology, is compromised. The A β - quantity, however, is not affected. On the other hand, A β - quality shows an increased trend towards oligomer-formation. A variety of possible explanations for these phenomena are presented. Summarizing, no significant evidence was found for a causal link between hypoxia and A β - protein depositions in AD.

Abkürzungsverzeichnis (List of abbreviations)

A β	amyloid- beta peptide
AD	Alzheimer's disease
APOE	apolipoprotein E
APP	amyloid- beta peptide precursor protein
ATP	adenosine triphosphate
BACE	Beta- amyloid cleaving enzyme
BBB	blood brain barrier
BSA	Bovine serum albumin
c	control
CIA	Central Intelligence Agency
CNS	central nervous system
CSF	cerebrospinal fluid
DAPI	4',6-diamidino-2-phenylindole
DMEM	Dulbecco/Vogt modified Eagle's minimal essential medium
DNA	deoxyribonucleic acid
EDTA	Ethylenediaminetetraacetic acid
ELISA	Enzyme-Linked Immunosorbent Assay
GDP	gross domestic product
HCT	hematocrit
HE staining	Hematoxylin and Eosin staining
HIF	hypoxia-inducible factor
HRE	HIF- responsive element
H/ Hx	hypoxia
Ig	immunoglobulin
IGF2	insulin- like growth factor 2
LTP	long- term potentiation
MPS	mononuclear phagocyte system
NFT	neuro-fibrillary tangles
NO	nitric oxide
N/ Nx	normoxia

O.D.	optical density
OR	odds ratio
PAGE	polyacrylamide gel electrophoresis
PBS	phosphate buffered saline
PBTriton	Triton reagent added PBS
PFA	paraformaldehyde
PSEN1/2	presenilin1 and 2
PVWD	periventricular white matter damage
RAGE	receptor for advanced glycation end products
ROS	reactive oxygen species
SDS	Sodium dodecyl sulfate
Syst- Eur trial	Systolic Hypertension in Europe
tg	transgenic
TLR2	Toll- like receptor 2
TNF	tumour necrosis factor
US	United states
VEGF	vascular endothelial growth factor
WB	Western blot
WHO	World Health Organisation
wt	wild- type
XTT	2,3-bis-(2-methoxy-4-nitro-5-sulfophenyl)-2H-tetrazolium-5-carboxanilide

Introduction

1. Alzheimer's Disease

Cognitive decline with age has long been recognized as an issue in human society, even being a problem to be addressed in lawmaking as early as 500 B.C. by Solon, a Greek judge. But for long, it was considered a routine part of the aging process, with Plato and Aristotle stating that old age and mental failure were inseparable. Pythagoras reckoned it fortunate that few people arrive at such an advanced age (Berchtold et al., 1998). Since then, things have changed. In 1907 Alois Alzheimer published a case report that, in line with his fellow investigators at the time, started to see the observed condition of his patient as a disease, rather than an unfortunate property of old age (Alzheimer, 1907). This was a true turning point as cognitive impairment was beginning to be considered pathological rather than physiological and thus inevitable. However, roughly 100 years of investigation in the field have not yielded satisfying results yet, neither for treatment nor for cure. Nowadays, this issue gains increasing importance due to a rising life expectancy in the Western world.

1.1 Clinical Appearance

Alzheimer's Disease (AD) is a neurodegenerative disease of the elderly, both progressive and fatal. There is however a rare form of the disease (early- onset AD) of particular genetic background which places the disease onset earlier in life. Amongst the most common clinical features of AD are amnesic memory impairment, language deterioration and visuo- spatial deficits. In short, AD constitutes one possible pathology that eventually causes dementia, which differs from the first in that it is a clinical finding. In later phases motor and sensory abnormalities, gait disturbances and seizures do occur. Patients show behavioural alterations and experience a progressive impairment of daily living (Cummings, 2004).

Two forms of AD are to be distinguished: sporadic (late- onset) AD and early- onset AD, a subcategory of which is familial AD (Fig. I01). Early- and late- onset refer to before and after the age of 65 years, respectively. By prevalence, late- onset AD is 10- 20 times more common than early onset AD (Mayeux, 2010). Familial AD accounts for about 50% of all early- onset AD cases. The term "familial" refers to the fact, that affected individuals develop the disease due to genetic predisposition. About why the other 50% develop the disease earlier than usual little is known (Mayeux, 2010).

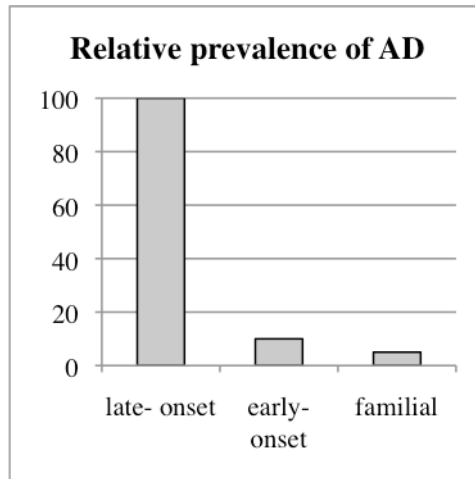


Fig. I01: Different forms of AD and their relative prevalence.

1.2 Epidemiology

AD has grown into a mayor public health issue as life expectancy rises constantly in developed countries over the last 50 years. The number of affected individuals increases with the progression of age, with prevalence roughly doubling every five years after 60 (Cummings, 2004). The following figure (Fig. I02) illustrates this for individuals from a general population in the West (WHO, <http://www.searo.who.int>).

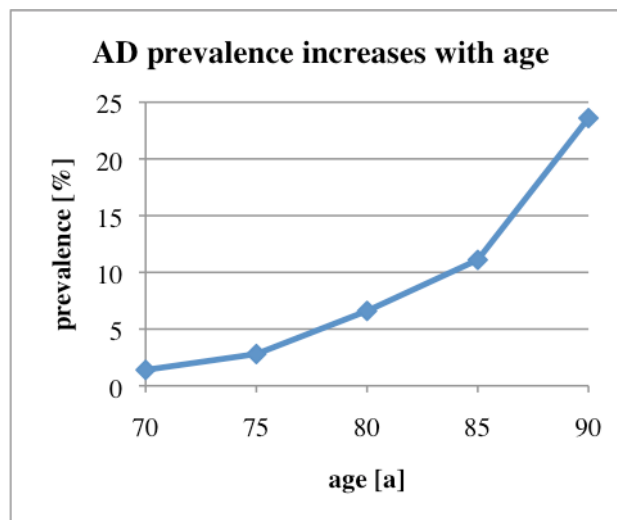


Fig. I02: According to statistical data from the World Health Organisation (WHO), the AD prevalence increases dramatically with age, doubling every five years from 60 years onwards.

In the US, out of 300 million citizens (U.S. Census Bureau, Report 2000), 5.3 million live with AD, which makes a 1.7% of the total population. Every 70 seconds somebody develops AD, the disease ranks 7th as cause of death, and 148 billion dollars are spent annually on medical care for AD patients and those with other dementias, which equals 1% of the gross domestic product (GDP) (CIA, World fact book). While cancer therapy evolves and offers

cures to a variety of tumours, no AD case has been cured since its discovery over 100 years ago. Effective symptomatic treatments are also still on the wait.

1.3 Pathophysiology

Histological features of patients' brain samples include the accumulation of the self-combinatory Amyloid- beta peptide ($A\beta$) in so called plaques, neuronal loss in selected brain regions and hyper-phosphorylated tau-protein in structures also referred to as tau- or neurofibrillary tangles (Blennow et al., 2006; Querfurth et al., 2010).

Where does $A\beta$ come from? Amyloid- beta peptide precursor protein (APP) is localized at the cellular membrane. It is cleaved in two major steps by proteases called secretases, leading to various products. Depending on which of the three α , β and γ -secretases consecutively cleaves APP, the process is amyloidogenic or not. To be more specific, if APP is cleaved first by β -secretase (also known as BACE, Beta- amyloid cleaving enzyme) and then by γ -secretase (a complex formed by various components), one of the products is $A\beta$ (Chow et al., 2010). The cleavage site of the γ -secretase is not precise and results in $A\beta$ protein variants with 39 to 43 amino acids, but mostly $A\beta_{1-40}$ and $A\beta_{1-42}$ with 40 and 42 amino acids, respectively.

There is no consensus concerning the physiologic functions of APP and $A\beta$. It is however likely that they exist, since pathology cannot exist for pathology's sake. APP is seen as a complex signalling center with multiple functions. Its main responsibility is believed to lie in the development of the nervous system and, through $A\beta$ as signalling molecule, in synapse suppression (Kim et al., 2006).

Efforts to understand the $A\beta$ related pathology can be divided in two main fields: research that focuses on genetic modifications to study disease outcome, and investigations focusing on biochemical properties of the $A\beta$ protein and interactions with itself and other players.

1.3.1 Genetic base

From the genetic viewpoint, AD is a heterogeneous disorder, with both familial and sporadic forms. After advanced age, a positive family history is the second most relevant risk factor for AD- like dementia (Selkoe et al., 2002b). APP is located on chromosome 21, which explains why patients with Down's syndrome show signs of early-onset AD by a gene dosage effect. Furthermore, various missense mutations have been characterized in the APP gene. They result either in more efficient cleavage by β -secretase and thus higher levels of $A\beta$, or modify the ratio $A\beta_{1-40} : A\beta_{1-42}$ in favour of the latter. Further mutations were localized to

presenilin1 and 2 (PSEN1/2) as part of the γ -secretase complex, which results in a gain of function, modifying cleavage towards a selective surplus in the production of A β 1-42 (Selkoe, 2002a). One of the factors not involved in A β processing but genetically associated with AD is the ϵ 4 allele of apolipoprotein E (APOE) (Corder et al., 1993; Poirier et al., 1993). The risk for AD rises three-fold in heterozygous and 15-fold in homozygous individuals (Farrer, 1997). The allele affects the age of onset by ten years per copy (Meyer et al., 1998). The exact mechanism responsible for this observation is still under investigation.

1.3.2 Protein base

The most abundant forms of A β - protein are A β 1-40 and A β 1-42 with 40 and 42 amino acids, respectively, in a ratio 10:1 (Rauk, 2008), with A β 1-40 as the predominant form found in cerebral blood vessels and A β 1-42 mostly situated in the brain parenchyma (Glenner et al., 1984; Kawarabayashi et al., 2001; Alonzo et al., 1998). An illustration of the APP is given in Fig I03.

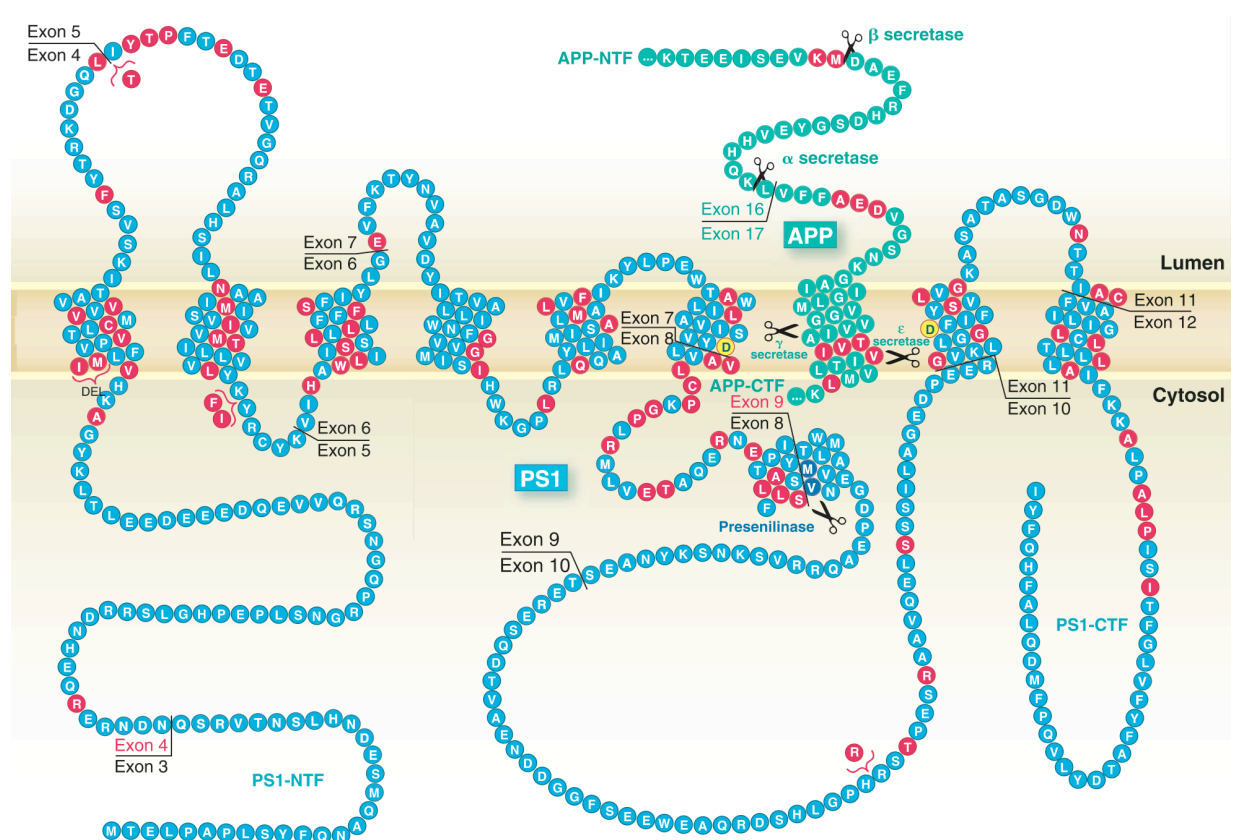


Fig. I03: Illustration adopted from Hardy et al. (Hardy et al., 2002); Shown is the processing of APP. Blue circles illustrate the amino acid sequence of APP. Red circles indicate mutations, known to cause familial AD. Scissors indicate cleavage sites for the various secretases and one protease.

Changes in the ratio in favour of the 42 amino acid isoform are associated with a more detrimental disease progression, which can in part be explained by the two additional hydrophobic amino acids in A β 1-42. One of the properties of A β is its capability to assemble with its own kind, owing to a self-recognition site at A β 12-23 (Tjernberg et al., 1997). It is consensus that neither the monomer (4.7 kDa), nor high molecular weight aggregates known as fibrils, are responsible for the neurotoxic effects associated with A β . Instead defects appear to be mediated by small oligomers, in the range of tetramers to 56 kDa (Lesne et al., 2006). To explain this further, the oligomer is a structure formed by aggregation of the monomer, self-assembling A β - protein. Various oligomers accumulate to even bigger structures called fibrils. The histologic correlate is the typical plaque structure found in AD brains. Summarizing, the above mentioned terms are referring to different grades of aggregation.

Typical effects observed are neurotoxicity and the subsequent suppression of long-term potentiation (LTP) required in memory formation (Lambert et al., 1998). Furthermore, memory impairment through various other mechanisms has been observed (Rauk, 2008; Lesne et al., 2006). It is thought that after A β secretion and oligomer assembly, these structures are either degraded or directed into formation of less toxic fibril aggregates and plaques (Cohen et al., 2006; Morimoto, 2006). These are then affronted, limited and digested by microglia (Napoli et al., 2009). This concept is supported by findings, that accelerating fibrillization lowers oligomer load, correlating with reduced functional deficits (Cheng et al., 2007). In support of this, plaque bearing mice with reduced oligomer levels showed an intact memory, unlike their littermates with normal levels of oligomers and memory deficits (Lesne et al., 2008). Interestingly, and somewhat unintuitive, A β - monomers have been reported neuroprotective (Giuffrida et al., 2010).

1.3.3 Conclusion

Integrating these findings, an “amyloid cascade theory” was formulated. Thereby, changes in A β metabolism lead to increased A β - protein quantities. This triggers a deleterious cascade: initial oligomer formation leads subsequently to synaptic dysfunction, resulting in inflammatory responses and plaque formation, followed by neuronal injury, dysfunction and death and consequent neurotransmitter deficits. These processes reinforce each other, and the cumulative effects are dementia and other cognitive clinical observations made in AD patients (Selkoe, 2002a). A figure adapted from this publication (Fig. I04) illustrates the cascade:

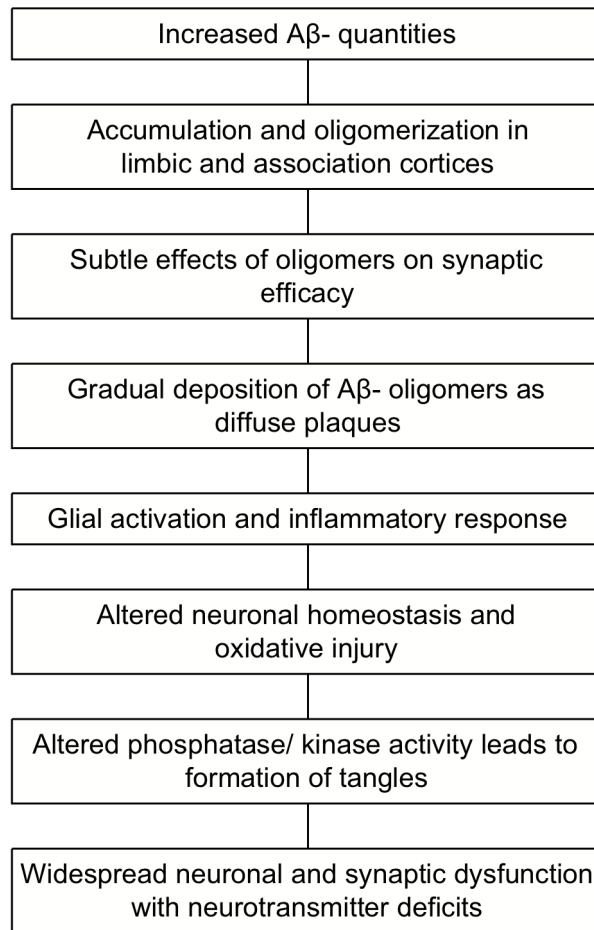


Fig. I04: The "amyloid cascade" according to Selkoe et al.: Accordingly, increased A β - protein quantities result eventually in widespread neuronal and synaptic dysfunction. Furthermore, the processes portrayed reinforce each other in complex and only partially understood ways.

2. From Risk Factors to Hypotheses

In this section, in addition to the non-modifiable genetic risk factors described in chapter 1, several potentially plastic risk factors for dementia will be introduced. The question posed here is: Given no genetic disposition and a similar familial history of AD, why do some people develop the disease while others don't? This review will focus on vascular alterations and hypoxia as possible pathogens (Khan et al., 2008) and develops the working hypothesis.

2.1 Non-Vascular Risk Factors

A wide range of risk factors has been reported for AD. For simplicity's sake, non-vascular ones will only be listed. Higher risk for AD correlates with: high homocysteine concentrations in serum, smoking, alcoholism, high serum cholesterol, high intake of saturated fat, diabetes mellitus, head injury, menopause, migraine, lower education and depression (de la Torre, 2004). Many of these are also risk factors for cerebrovascular diseases, a fact which indicates

that pathogenic mechanisms for AD and cerebrovascular diseases may be connected (Iadecola, 2004).

2.2 *Vascular Risk Factors*

The focus will now be put on vascular risk factors that have been found associated with AD. Again, findings will be listed without provision of a specific conceptual framework.

One study investigated the type and number of brain pathologies that were present in patients with dementia. The question posed was, whether the underlying pattern of brain pathology influenced a patient's developing dementia or not. The compared groups had either a single brain pathology, such as AD, or presented a "mixed" picture, say AD and stroke. In the dementia group, over half of the patients presented a multiple, mixed diagnosis. For example the combination AD and infarctions combined was observed in 38% of dementia patients, while 30% had singularly "pure" AD. In those without dementia, 80% had no or only one diagnosis of associated brain pathology. Multiple diagnoses of brain pathologies show an odds ratio (OR) of 2.8 for dementia. This means that patients with various brain irregularities are nearly three times more likely to develop dementia (Schneider et al., 2007). This notion is supported by similar findings of faster dementia progression in AD patients with coexisting cerebral infarctions compared to individuals presenting only "pure" AD pathology (Sheng et al., 2007). Further support comes from the so called Nun-study, where small ischemic lesions, which by themselves would not alter cognition, aggravated dementia substantially in combination with AD (Snowdon, 2003). As shall be discussed later, the above mentioned line of evidence forms the basis for the working hypothesis of this study.

Hypertension is associated with a higher risk for the development of AD. Evidence was found in the Systolic Hypertension in Europe (Syst- Eur) trial. Patients under antihypertensive treatment had a relative risk of 0.47 for dementia, compared to the non- treated group. (Patterson et al., 2008; Forette et al., 1998).

In a mathematical approach performed by Goh et al., AD was found genetically associated with hypertension and myocardial infarction (Goh et al., 2007).

Over two-dozen vascular risk factors (de la Torre, 2008) have thus far been related to AD by various epidemiological studies, amongst them being the Rotterdam study, the Kungsholmen project, the Framingham study, EURODEM, FINMONICA, the Honolulu- Asia study and the PROCAM project (Breteler et al., 2000; Aguero-Torres et al., 2006; Ruitenberg et al., 2005; Elias et al., 1993; Ivan et al., 2004). The recent EVA study showed that patients under

vascular care showed less progression of white matter disease, common in AD, compared to control subjects without treatment (Richard et al., 2010).

Furthermore, twin studies have provided hints concerning the magnitude of non-genetic risk factors. Monozygotic twins have two times the incidence of AD compared to dizygotic twins (Raiha et al., 1996). Interestingly, the incidence ratio of the two groups for vascular dementia is one. Monozygotic twins show higher concordance rates than dizygotic ones, confirming the major role that genetic predisposition plays in AD development (Bergem et al., 1997). However, since genetic background is not sufficiently explicatory, the need to identify environmental components of AD pathogenesis remains of great importance. Another twin study comparing the relative importance of heredity and environment in AD development confirmed the major role of genetic predisposition, but found that vascular dementia was mainly caused by environmental factors, with heredity playing a minor role (Bergem et al., 1997). This is interesting considering that AD and vascular dementia are sometimes described as opposite ends of the spectrum of one integrative disease mechanism (Roman et al., 2004). Further vascular risk factors are congestive heart failure, cardiac arrhythmia, thrombotic episodes, atrial fibrillation, atherosclerosis and hemodynamic abnormalities (de la Torre, 2004).

Summing this up, general findings such as ischemic and hypoxic tissue conditions are associated with a worse prognosis of dementia. They act both as cause and consequence in most of the above described pathologies. However, little is known about the direct influence of hypoxia on AD development and progression (Khan et al., 2008).

3. Defining hypoxia

The following chapter will introduce the basic concepts of oxygen sensing.

3.1 Oxygen sensing and signalling

The body has various specialized tissues through which it senses oxygen, for example glomus cells, the carotid body and neuroepithelial bodies in the lungs amongst others. Together they constitute a specialized homeostatic oxygen-sensing system, responding primarily to acute hypoxia, the physiologic range in oxygen tension ranging roughly from 40 to 100 mm Hg in the adult, while all tissues respond to severe hypoxia (Weir et al., 2005). At the molecular level, the hypoxia-inducible factor 1 (HIF-1) pathway is the key regulatory route by which gene expression is modified in order to facilitate adaptation and thus survival of cells under hypoxic conditions (Ke et al., 2006). Although other HIFs exist, we shall focus here on HIF-1.

It is an oxygen- sensitive transcriptional activator, inducing genes that participate e.g. in angiogenesis, iron metabolism, glucose metabolism and cell proliferation. HIF- 1 consists of two constitutively expressed subunits: a β - subunit and an oxygen- regulated α - subunit. Both need to associate as a heterodimer at a HIF- responsive element (HRE) at the target gene promoter to induce gene transcription. Through post- translational modification the α - subunit is degraded rapidly under normoxia. To be more specific, HIF prolyl- hydroxylases hydroxylate conserved proline residues of the α - subunit, allowing their ubiquitinylation and subsequent protein degradation by the proteasome. However, this occurs only under normoxia, since the hydroxylase is dependent on oxygen as a co- substrate. Under hypoxia it is inhibited, which stabilizes the α - subunit. It then interacts with other co- activators, most importantly HIF- 1 β , and ultimately binds to the HRE. This gives way to gene transcription (Ke et al., 2006; Rey et al., 2010; Kaelin et al., 2008).

This results in a variety of modifications. On a cellular level glucose metabolism is switched to oxygen- independent glycolysis (Dang et al., 1999). This results in a yield of only two adenosine triphosphate (ATP) per molecule glucose instead of 38 obtained through oxygen- dependent glycolysis. This switch occurs because under hypoxia oxydative phosphorylation does not occur. ATP- deprived cells elevate their ability to generate ATP through an increase in glucose uptake and an upregulation of enzymes such as Lactate dehydrogenase (Wenger, 2002). Another reaction to low oxygen supply is induction of growth factors such as insulin- like growth factor 2 (IGF2), which downstream causes cell proliferation and survival (Semenza, 2003). On a bigger scale, hypoxic conditions also cause angiogenesis, because expression of the vascular endothelial growth factor (VEGF) is enhanced by HIF (Conway et al., 2001).

3.2 *Molecular findings linking HIF to AD*

Hypoxic conditions have been shown to upregulate BACE1 expression and activity, resulting in an increased A β - protein production, both in vitro and in vivo (Sun et al., 2006). Furthermore, HIF1 has been shown to bind the BACE1 promoter on a HRE, thus regulating gene expression (Zhang et al., 2007). Another study confirmed these findings, extending the hypoxia- mediated upregulation by another mechanism: the formation of reactive oxygen species (ROS) (Guglielmotto et al., 2009). Another component of the γ - secretase complex, called APH-1A has been shown to be hypoxia- responsive too, again with a HRE in its gene's promoter sequence, culminating in hypoxia- induced, increased A β - protein formation (Wang et al., 2006). In another study, using in vitro neural cultures, it has been shown that A β -

protein is able to activate the HIF1 transcription factor, which acts as a neuroprotective mechanism for the corresponding cells. It produces changes in glucose metabolism like an increased glucose flux, making the cells more resistant to the A β - protein toxicity (Soucek et al., 2003). This at first paradoxical finding supports the idea, that the effects of the A β -protein depend on its conformation, i.e. monomer, oligomer or fibril. However, because of this adaptation, or conditioning, the A β - resistant neuron population is more susceptible to glucose starvation, the latter being a feature of various vascular pathologies (Soucek et al., 2003).

4. Microglia and AD

The first line of defence that the body has to react against the plaque depositions is a glial subpopulation called microglia, believed to play an important part in neurodegenerative conditions. This is why we focused on this population in our experiments.

4.1 Origin, innate immunity, function, phenotype, activation

Although microglia had been described before, Pio del Rio-Hortega, a student of Santiago Ramón y Cajal, is generally considered the „father of microglia“ for his pioneering work in the field. These cells constitute 10% of the central nervous system's (CNS) cell population (Heneka et al., 2007), form part of the mononuclear phagocyte system (MPS) and represent a part of the innate immunity of the CNS (Ransohoff et al., 2009). Cells that are functionally equivalent to microglia can already be found in the invertebrate CNS, e.g. in leech (*Hirudo medicinalis*) (Morgese et al., 1983). Microglial cells occupy non-overlapping territories in the brain parenchyma, which they continually palpate and thus monitor through their numerous processes. In effect, the microenvironment around an individual cell is screened every couple of hours by this highly dynamic mechanism (Nimmerjahn et al., 2005).

Where do microglia originate? At early stages of development (embryonic day 8 in mice), before the development of vasculature, myeloid cells can be found in the CNS with proliferative capacities (Alliot et al., 1999). However, their origin (i.e. lineage) remains unclear. Postnatal, circulating cells of myeloid origin have been observed to enter the brain (Perry et al., 1985). It is not established, however, to what extent these cells persist to form part of the population of microglia observed in adulthood. Generally, microglia are believed to be a long-lived population of tissue macrophages, not unlike Kupffer cells in the liver (Ransohoff et al., 2009).

But what does long- lived mean? As will be discussed later, it is also of importance to know whether microglia age, in the sense that their correct and adequate function might be compromised. Dystrophic microglial cells accumulate in the aging human brain, suggesting that this cell population undergoes progressive deterioration. It is suggested that diminished replenishment and increased vulnerability contribute to the phenomenon (Streit, 2006). Since microglia are essential for the maintenance of normal brain function, deterioration of this cell population might be a crucial factor in the development of age- related neurodegenerative diseases such as AD.

It needs further clarification whether the microglial population is morphologically uniform, since functionally it is highly heterogeneous (Gordon, 2003). This reflects the plasticity and versatility of this cell population in response to a wide array of signals. Microglia acquire different phenotypes according to stimuli, and their phenotype has to be seen as a point in a spectrum of possibilities, whose extremes pose the M1 and M2 activation profiles: Microbial compounds and pro-inflammatory cytokines cause the so- called M1 phenotype, marked by the production of pro-inflammatory cytokines and free radicals (Michelucci et al., 2009). The M2 phenotype, also called alternative activation, is less well defined, consisting of at least two subgroups separated through their expressional profile. However, it is thought to be anti-inflammatory (Mosser, 2003). Interestingly, there is evidence that a phenotype switch takes place as Alzheimer's disease related pathology progresses. In an animal model, microglia switch from an alternative, neuroprotective activation profile at the beginning of A β - pathology, to a classical M1- like, potentially neurotoxic phenotype at advanced stages of the disease (Jimenez et al., 2008). Furthermore, A β - fibrils and oligomers seem to stimulate microglia in different ways, leading to discrete secretory changes (Sondag et al., 2009). The receptors involved are scavenger receptors (including CD36), receptor for advanced glycation end products (RAGE), Toll- like receptor 2 (TLR2) amongst others (Lucin et al., 2009). This implies that the A β - protein can, dependent on the context, stimulate a variety of pathways and thus reactions. This in turn partially explains why, from a clinical point of view, in many neurodegenerative diseases it is not entirely clear whether inflammation and microglial activation are deleterious or beneficial (Lucin et al., 2009).

4.2 *Microglia and hypoxia*

Microglia play an important part in various clinical contexts and conditions, e.g. periventricular white matter damage (PVWD). It is one of the major causes of neurological impairment in premature newborns. Its aetiology, although being multi- factorial, is thought

to be linked to a state of hypoxia- ischemia through birth asphyxia (Kaur, et al., 2009), findings that have been confirmed in humans (Black et al., 2009). In this clinical context, microglia are appointed a critical role in PVWD.

Accordingly, activation of microglia (i.e. inflammation) through hypoxic conditions could cause bystander injury to other CNS cells. In animal experiments, increased numbers of activated microglia have been observed to be present in the white matter of asphyxiated animal fetuses (Mallard et al., 2003).

Glial activation is a consequence of hypoxia (Suk et al., 2004). The resulting oxygen deprivation has been found to induce shedding of nitric oxide (NO) and tumour necrosis factor (TNF- α) in enriched microglial cultures, and cellular death after 12 hours exposition (Wang et al., 2007). How does this transform to the clinical context? Neither NO shedding after glial activation nor hypoxia cause wide neuronal damage by themselves. However, when combined, extensive neuronal death is the consequence (Mander et al., 2005). Microglia through inflammatory responses thus have the potential to cause neuronal damage. Hypoxic conditions seem to function as a possible trigger mechanism.

Materials & Methods

1. Animals

A murine model of Alzheimer's disease (AD) was used, namely the Tg(APP^{swe}, PSEN1^{dE}). In humans, various mutations in key proteins are associated with familial AD. Animal models mime these in order to mimic the related pathology. More specifically, double transgenic mice were used. First, they express a chimeric mouse/human amyloid precursor protein (mo/huAPP) presenting the Swedish mutations (Haass et al., 1995) K595N/M596L, meaning that in the transgenic animal lysine at position 595 is changed for asparagine, and methionine for leucine at position 596, the location being before the A β sequence. The reason a chimeric protein is employed is because in mice no naturally occurring AD like disease has been observed, because apparently huAPP homologues in mice, APLP1 and 2, have different properties. Second, these animals present the mutation PSEN1^{dE9}, meaning that exon 9 is deleted in the sequence of presenilin 1, a major constituent of the γ -secretase complex. This mutation has been observed to selectively augment the APP cleavage product A β ₁₋₄₂ (Jankowsky et al., 2004). A combinatory transgenic model, including both mutations for APP and PS1, has been described to show early amyloid deposition, thus being valuable as an animal model for AD (Borchelt et al., 1997; Savonenko et al., 2005). Both mutated proteins are under expression control of the prion protein promoter (Prnp) thus being limited to expression within the central nervous system (CNS). Visible amyloid deposits occur as early as 6 months, and various AD related pathologies have been described (Garcia-Alloza et al., 2006; Yan et al., 2009).

Animals were obtained from Jackson Laboratory (Strain name: B6.Cg-Tg(APP^{swe}, PSEN1^{dE9})85Dbo/J, stock number 005864).

2. Genotyping

The material for DNA extraction was cut fingers from the process of numbering the animals. According to the manufacturer's instructions, the DirectPCR DNA Extraction System (Viagen) was employed, with the modification of added proteinase K (Roche). Amplification was carried out using Dominion MBL-taq polymerase. Primers were designed to match the APP coding sequence (forward 5'- CTT GTA AGT TGG ATT CTC ATA TCC G- 3', reverse 5'- GAC TGA CCA CTC GAC CAG GTT CTG- 3'). The electrophoresis was carried out according to standard procedures.

3. Hypoxia treatments

Two groups of animals were compared - those under hypoxic exposure and those under normoxia, corresponding to 8% and 21% oxygen respectively, for 20 consecutive days. Both groups were kept in their particular setting in a specially constructed oxygen-variable chamber (Coy Laboratory Products). No preconditioning of the hypoxia group was undertaken. Atmospheric conditions were kept stable and automatically monitored for changes (gas guard, Thermo Electron Corp.), in which case the system re-established the experimental conditions (oxygen controller, Coy Laboratory Products). Furthermore, the oxygen concentration was checked manually every second day (combustion test kit, Bacharach), whereby a difference of 0.5% from the above-mentioned value was still considered acceptable. Humidity inside the chamber was always kept below 80% using absorbing silicon, as otherwise the animals would have died. CO₂ was filtered through a special pump system employing sodium, as part of the specially designed chamber. All parts of the system and reagents were replaced according to their functional state. Access to the chamber for feeding and cleaning occurred through an air lock leaving the conditions in the chamber unaffected. Light, feeding and cleaning cycles were kept uniform for all groups. All treatments were in accordance with ethical standards of the University of Sevilla (Spain) and approved by the Committee of Animal Use for Research of the Malaga University (Spain) according to the European Union Regulations.

4. Tissue preparation/ HCT measurement

In order to confirm the exposure to hypoxia or normoxia, the hematocrit (HCT) of all animals was measured.

Animals were taken from the chamber and immediately sacrificed by injection with Thiobarbital (Braun, 0.15 mL, if this did not suffice, further injections were administered). No reflexes to pain, both in tail and eye, were taken as indicator of death. Animals were then fixed to a board with needles and blood was drawn for HCT measurements. The following surgical procedure was undertaken to get access to blood from the right coronary auriculum for analysis: After disinfection with 70% ethanol, skin was cut open epigastric to suprasternal, then moved aside through subcutaneous incisions. Subsequently an infracostal horizontal incision opened the abdominal cave. It was important to cut in on the right-hand side of the animal as this assured no damage to the heart or associated structures. From here, the diaphragma was dissected, opening the thoracic cave. Then, the ventral costal cage was

removed, exposing the heart. An incision in the right auriculum was made, while hearts were still beating, and released venous blood was collected in a capillary. It was then sealed with plasticine and centrifuged for 5 min at 5000 rpm. To calculate HCT, the length of the capillary part with solid matter was divided by full capillary length (parts sealed with plasticine were excluded from calculation).

After blood withdrawal, animals were decapitated by guillotine. Skin was then removed from the skull with a median incision. Using pliers the skull was opened at point Bregma. With the same tool the skull was carefully removed around the brain. This was then put into a Petri dish filled with PBS at 4°C. Brains were sliced in half, with the left hemisphere being put into liquid nitrogen and later stored at -80 °C for protein analysis experiments, while the right was put in PFA 4% at 4°C. Total surgery and storage was exercised within 10 minutes after the declared death of the animal.

For paraffin fixation the tissue was placed 12 h in PFA 4% and stored at 4°C. Then, samples were transferred to ethanol 70% until paraffin inclusion 9h later. Half brains were fixed using a uniform protocol automatically carried out by an Inclusion automat (ASP300S, Leica). Paraffin blocks were stored at 4°C until further processing. Slicing was done on a microtome (RM2125RT, Leica) at 20 µm.

5. Immunohistochemistry

All sections were deparaffinized with help of xylene and a row of decreasingly concentrated ethanol and finally water (2x 100% 5', 90% 5', 80% 5', 70% 5', 3x distilled water total 5').

5.1 Aβ1-42 staining

Two different methods were used for plaque staining. An antibody based approach was employed considering various optimization techniques (Cummings et al., 2001). A second approach included the reagent Thioflavine-S, described below. First, peroxidase remaining activity was terminated by incubation with H₂O₂ at 3% for 15 minutes, followed by a wash step (3 times 5 minutes in distilled H₂O). Then antigen retrieval was performed in a bath of 99% formic acid for 3 minutes, followed by another wash step. Subsequently, slices were blocked in IHC blocking solution (PBS with 5% skim milk) for 1 hour at room temperature. Afterwards, the primary antibody in blocking solution was added and left to incubate at 4°C over night (rabbit polyclonal Aβ1-42, Calbiochem, 1:100). Following a wash step with 0.1% Triton reagent (Sigma) added PBS (from hereon referred to as PB-Triton), the secondary antibody solution (IgG goat anti-rabbit, Dako) in blocking solution was put and left for one

hour at room temperature in a wet chamber. After another wash with PB-Triton, revelation procedure was carried out as described in the manufacturer's instructions of the EnVision + System-HRP kit (Dako) using the DAB chromogen. After 2 minutes exposure the chromogen was inactivated with an additional wash. Sections were mounted with aqueous mounting medium (Dako), left to dry and sealed with colourless nail polish (Barbie Manicure Set).

5.2 *Iba1 staining*

Iba1 is an EF-hand calcium-binding protein specifically expressed in macrophages and microglia, that was employed as a target to evaluate the microglial population. After deparaffinization of tissue sections, intrinsic peroxidase activity was inactivated by incubation in 3% H₂O₂ for 30 minutes and a subsequent wash step (distilled water 3x 5'). Antigen retrieval was performed by incubation with 10 mM citric acid (pH 6) at 95°C for 20 minutes followed by 45 minutes at 4°C. After another wash step, unspecific antigens were blocked with a solution of skim milk (5%) in PBS for 1h. Then, the primary antibody (Iba1, polyclonal rabbit, Wako) in skim milk solution (1:500) was applied for 1h at room temperature. Following a wash step with PB-Triton, a revelation kit was used to stain the marked areas (EnVision+System-HRP/DAB, anti-rabbit, Dako) with 1h incubation with the secondary antibody and 4 min DAB exposure (Fig. MM01). Sections were mounted and sealed as described above.

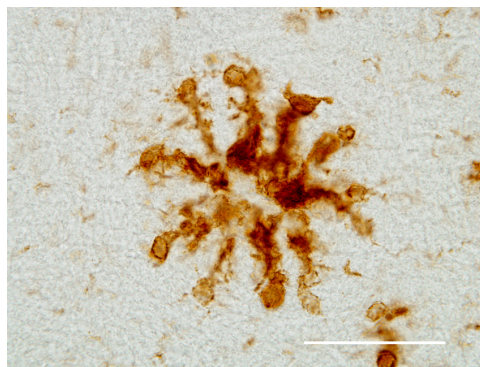


Fig. MM01: Iba1 stained microglia surrounding what appears to be a plaque. Scale is 50 μ m.

6. *Other staining techniques*

6.1 *Thioflavin-S staining*

The fluorescent reagent Thioflavin-S (Sigma) reacts with β -sheet structures, and thus recognizes A β -plaques as well as neuro-fibrillary tangles (NFT). Vessels were observed to show high autofluorescence under this type of staining due to unknown properties, which

limited its use for quantitative purposes. It was however effective for double staining procedures (Fig. MM02).

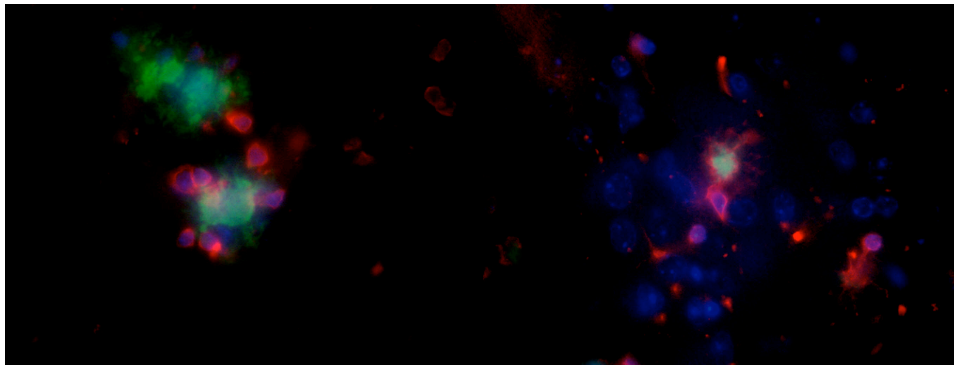


Fig. MM02: triple- staining with Iba1(microglia), Thioflavin-S (plaques), DAPI (nuclei): Microglia surrounding plaques and limiting their expansion

Pre-stained slices were washed and then incubated with 0.05% Thioflavin-S in 50% ethanol for 8 minutes in darkness. This solution was then filtered (filterunit SteriCup, Millipore). Afterwards the sections were treated 3 times 10 seconds with 80% ethanol to remove auto-fluorescent background noise, followed by a similar wash step with distilled water. Fluorescence Mounting Medium (Dako) was used for mounting. The signal was finally obtained under UV-light (Fig. MM03).

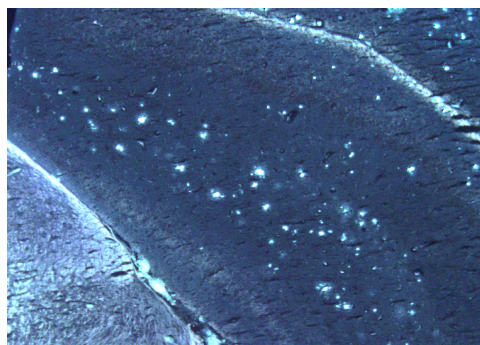


Fig. MM03: Plaques in the hippocampal formation, Thioflavin-S stained

6.2 Prussian staining

This technique was used to stain ferric iron, as can be found in hemorrhage. This method was used to assess whether there was excessive extra-vascular bleeding under the treatment conditions. After deparaffinization and rehydration, sections were stained for 20 min in a solution made up in equal parts of a: 20% aqueous solution of hydrochloric acid and b: 10% aqueous solution of potassium ferrocyanide (protocol from IHCworld). Counterstaining was done with nuclear fast red (Sigma) for 5 min.

6.3 *Hematoxylin and Eosin staining*

In order to evaluate structural changes under treatment, especially angiogenesis, Hematoxylin and Eosin (HE) staining was employed. According to standard protocols, Accustain Harris' hematoxylin and eosin solutions (Sigma) were used.

7. *Cell Culture*

To obtain primary microglia populations, a procedure was employed that enriched these cells in the cell culture (Saura et al., 2003). The cultures obtained are mixed. But due to the lack of an established microglial cell line and our aim, to monitor the cells' response as close to their natural state as possible – for which the interaction with other cell types is also important – the usage of this method was decided on. It needs to be pointed out that the data obtained from such a culture, concerning their relevance for microglial properties, is restricted and still a matter of debate (Saura, 2007). Thus, one might want to call this culture type more exactly microglia- enriched cultures (Jimenez et al., 2008), as will be done from hereon.

Microglia- enriched primary cultures were prepared from newborn C57BL/6 mice (1–3 d, Jackson Laboratory). Animals were decapitated, and the cerebrum (telencephalon) removed. Then, while conserved in sterile PBS at 4°C, the meninges were removed under a microscope. For each cell seeding cycle this procedure was performed for all brains at a time to keep uniformity. Briefly, the dissected brains were treated for 5 min with DMEM-medium (Gibco) (with trypsin 0.25% + EDTA 1mM (Gibco)) at 37°C. During these 5 minutes incubation, the cells were mechanically dissociated three times using a pipette for gentle aspiration. The trypsin was stopped using complete DMEM/F12 (50:50, Gibco; added 10% FBS (Hyclone)). Subsequently, the debris was eliminated by filtration (cell strainer, 40 µm, BD Falcon) and the cells were seeded (250.000 cells/mL) in complete medium DMEM/F12, 10% FBS added L-glutamine (Gibco), nonessential amino acids (PAA), 1% gentamycin (Sigma) and penicillin-streptomycine (Sigma) on 12-well-plates (Nunc) pretreated with poly-D-lysine (Sigma). The cells were cultured at 37°C in humidified 5% CO₂/ 95% atmosphere, with medium being replaced every three days. Once a well had reached about 90% confluency, a mild trypsinization step was performed: 0.25% trypsin + EDTA 1mM was diluted 1:4 in raw DMEM medium (Gibco). It has been estimated that under these conditions the calcium concentration is higher than the sequestering capacity of the present EDTA. The non-sequestered free calcium partially inhibits trypsin (Saura et al., 2003). This results in the observed partial trypsinization. The culture was left for 20 min with the solution at 37°C. After a washing step with sterile PBS at 37°C, new complete medium was added, and cells

left to expand. In the protocol used, a yield of up to 98% microglia was reported (Jimenez et al., 2008), however, it was only possible to generate a mixed culture with 50% of the population being microglia (Fig. M04).

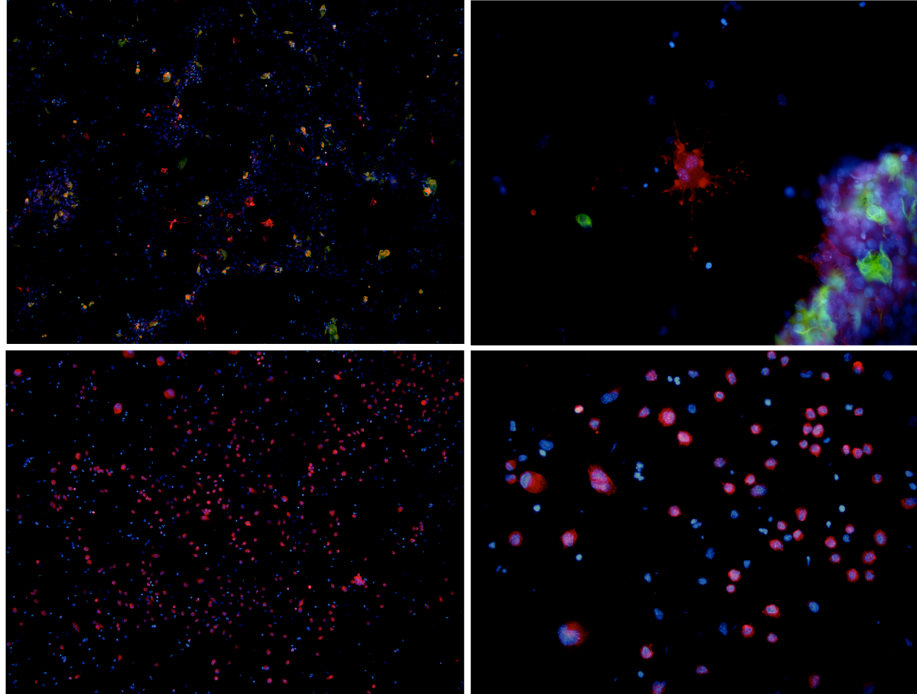


Fig. MM04: Primary, microglia- enriched cell cultures; directly after isolation (top two images) and after enrichment procedure (bottom two images)

8. Immunocytochemistry

For the identification of microglia the Iba1 antibody was used (see above, Immunohistochemistry). A small glass plate of 0.5 x 0.5 cm was prepared to be left in a well and overgrown by cells. Prior to that the glass was made sterile and incubated with poly-L-lysine for 2 h so that cells could attach. First, the well was cautiously washed with PBS. Then the platelet was incubated for 1 h with PFA at 4% at room temperature. After a wash step with PBS, antigen-block was done with skim milk solution, as described above. Subsequent incubation with the primary antibody in milk solution (Iba1, 1:500) was for 2 h. The fluorescent secondary antibody (AlexaFluor 568, 1:500 in milk solution, anti-rabbit, Molecular Probes) was left to bind for 1 h in darkness. Counterstaining of nuclei was done with DAPI (1:1000 in PBS, Sigma) (Fig. MM02 and MM04). For mounting, a special medium (Fluorescent Mounting Medium, Dako) was used.

9. Hypoxia treatment of cells/ XTT assay

Prior to treatment the cells were plated in a 96-well-plate (Nunc) at 8.000 cells per well and left one day to settle. Two groups were formed: cells under hypoxia (0.5% O₂, 5% CO₂) and those under normoxia (atmospheric conditions). The hypoxic exposition was possible through the use of an incubator with variable oxygen concentration (hypoxic chamber INVIVO2 300, Ruskin Technology) and controlled and adjusted with gas mixer q (Ruskin). Exposition times were 4, 24 and 48 hours respectively. The XTT assay (Roche) is based on the principle that live cells reduce tetrazolium salts into coloured formazan compounds (Scudiero et al., 1988), which can then be quantified through measurement of optical density (O.D.). It is commonly used as a procedure to measure proliferation and is thus an appropriate solution to quantify cells and assess their viability. The assay was carried out according to the manufacturer's instructions. O.D. was measured using a Multiscan Spectrum luminometer/spectrophotometer (Thermo Electron Corp.), right after addition to wells and then at the corresponding point in time. For analysis, measurements were corrected with this starting value ($value_x - value_0$). Experiments were repeated three times with eight wells for each time point and repetition. All measurements were later collected according to group, and the mean normalized to the mean value at 4 h normoxia.

10. Protein extraction and quantification

For protein extraction, first the wet mass of hemibrains was determined. They were then homogenized manually employing a Dounce grinder (Sigma) with 4x mass of PBS added including protease inhibitor cocktail (1:1000, Sigma) and phosphatase inhibitor (1:100, Sigma). An aliquot was centrifuged 10 minutes at 2000g at 4°C and supernatant was stored at -20°C and subsequently used for WB experiments. For ELISA sample preparation, 8.2M guanidine HCl/ 50mM Tris HCl solution was added to a final molarity of 5M. The prepared sample was incubated 4h at room temperature with casual mixing. After incubation, the sample was stored at -20°C until further use.

Sample concentrations were determined by the method of Lowry, using the kit DC Protein Assay (Biorad) following manufacturer's instructions. BSA was used as protein for the standard curve. A correlation coefficient of $R^2 > 0.997$ was considered acceptable.

11. Western blot (WB)

For polyacrylamide gel electrophoresis (PAGE) the Mini-protean system (BIORAD) was used. Electrophoresis was performed with electrophoresis buffers at 150 mV (Tab. MM01).

In the case of WB detection of A β protein, Tricine- SDS-PAGE had to be employed. This is because the target protein, due to its small size of 4.7 kDa, does not enter the gel with the electrophoresis protocol used for standard SDS-PAGE. Following instructions of Schägger, the protocol was modified (Schägger, 2006).

Acrylamide gels are characterized by two values: For one "x % T", which equals the total percentage concentration of acrylamide and the crosslinker bisacrylamide combined. The second value, "x % C" corresponds to the percentage concentration of the crosslinker relative to the total concentration. A gel of 16% T, 6% C and 6M urea was used. This led to a gel resolution of 1- 70 kDa. The high crosslinker concentration together with the added urea increases the resolution, especially of small proteins, further.

Furthermore, no SDS was added, as this would have denaturalized A β protein oligomers and fibrils. Our intention was to visualize the quantities of oligomers of different sizes.

	Anode buffer (10x)	Cathode buffer (10x)	Gel buffer (3x)
Tris (M)	1.0	1.0	3.0
Tricine (M)	-	1.0	-
HCl (M)	0.255	-	1.0
pH	8.9	~ 8.25	8.45

Tab. MM01: Buffers according to the Tricine- (SDS)-PAGE protocol described by Schägger.

Gels were subsequently transferred to PVDF membranes, which prior to use were activated with methanol. Employing a semi-dry transfer system (SIGMA) gels were transferred for 2 h using transfer solution (Tris 25 mM, glycine 192 mM and 20% methanol). Current in mA was calculated by membrane area in cm² times 1.2 as a fixed value.

Afterwards, the membranes were blocked for 1 h in blocking solution. Then the primary antibody in blocking solution was incubated overnight in a wet chamber (mouse monoclonal 6E10 from COVANCE 1:500) Then, membranes were washed 4 times in PBS supplemented with 0.1% Tween-20 (PBTween-20) for 5 min each turn, following incubation with the peroxidase-conjugated secondary antibody in blocking solution for 1 h at room temperature. After another washing step, signal detection was done using ECL PLUS Western Blot Detection System kit (GE HEALTHCARE).

12. Dot blot

For dot blots, 5 µg protein in 2 µL sample were applied directly onto a dry nitrocellulose membrane (Hybond) and left to air dry. Then the membrane was transferred to blocking solution for 1 h. Incubation with the primary antibody (A11, Invitrogen, 1:500) in blocking solution was over night at 4°C. Incubation with the secondary antibody, revelation and blot analysis was done as described for WB.

Signals from blots were visualized using a Typhoon Scanner (9400 variable mode imager, Amersham Biosciences), and subsequent image analysis and signal quantification was done with ImageQuant (Amersham Biosciences).

13. ELISA

This immunoassay was employed to detect levels of human Aβ₁₋₄₂. The principal is based on the quantitative detection of the target protein by its binding to specific antibodies, one coated onto a plate and one in solvent, the latter being detected by means of a horseradish peroxidase-labelled secondary antibody through substrate conversion. The intensity of the coloured product is directly proportional to the concentration of human Aβ₁₋₄₂ in the original specimen.

Thawed ELISA samples in guanidine 5M were diluted 1:50 in reaction buffer (BSAT-DPBS). This dilution factor was determined prior to experiments. It was taken into account that the final solution content of guanidine should not exceed 0.1 M since standard curve alterations were observed above (see manufacturer's instructions, ELISA kit, Invitrogen). After a subsequent centrifugation step at 16,000 g for 20 minutes at 4°C, the supernatant was carefully decanted and stored on ice until used for the assay.

For standard curve samples, lyophilized synthetic peptide was used (provided in kit). The protein powder was reconstituted (see corresponding buffer) to a concentration of 1 µg/mL, aliquoted and stored at -80°C until further use. For generation of the standard curve, buffer components and dilutions had to be the same as in samples of unknown Aβ₁₋₄₂ content. Since the test's upper detection limit is located at 1000 pg/mL, the required dilution factor for samples was determined to be 1:100 in sample diluent buffer (provided in kit). The buffer used to generate the standard curve was adjusted accordingly. Serial dilutions yielded the linear standard curve through linear regression analysis and a correlation coefficient $R^2 > 0.995$ was considered acceptable. To all samples, both of known and unknown Aβ₁₋₄₂ content, protease inhibitor was added (1:1000).

In the actual procedure, standards, controls and samples were added to 8 well strips of a 96 well plate and incubated with the primary antibody 3 h at room temperature under constant shaking on a shaking block. After repetitive washing with the provided solution, the secondary antibody was incubated at room temperature for 30 minutes. After another washing step, the provided chromogen was added, and stopped after 10 minutes with the provided stop solution to not exceed an optical density (O.D.) of 2.0 to ensure linear measurements. O.D. was taken at 450 nm using the luminometer described above.

14. Plaque load estimation/ Stereology/ Microglia count

Hippocampal A β - protein 1-42 immunostaining from 8- and 14- month- old APP/PS1 mice was observed under an Olympus BX61 microscope using a 10x objective. Stereologic tools were from the Olympus CAST software package. Images were acquired with an Olympus DP70 high-resolution digital camera. The camera settings (white balance, light intensity etc.) were adjusted at the start of the experiments and throughout maintained for uniformity. Digital images (five sections per mouse) were analyzed using ImageJ software (NIH freeware).

The dentate gyrus was chosen as sample area for plaque load determination. Neuroanatomy was assessed using a Mouse Brain Atlas (Paxinos). In each animal, the first section where this structure reaches the ventral side of the brain was identified and taken as starting point. From here two sections, respectively caudal and ventral, were also taken into consideration.

The sample area (the dentate gyrus) was then manually outlined and the total area assessed using CAST software. A digital image was then taken off each section, with a constant 0.625 pixels per μm^2 . The image was then edited using ImageJ: After colour conversion to black-and-white (8-bit), the plaque area within the dentate gyrus was identified by bright-level threshold, the level of which was maintained for uniformity throughout the experiment. The gray-scale image was thus converted to a binary image, with only plaque areas remaining within the sampled dentate gyrus area. This image was compared to the original, and through the automatic selection process erroneously selected items were manually removed, such as unspecific or intracellular staining. Using the “Analyze Particles” option, and maintaining the same settings for uniformity, the plaque areas were analyzed for area, number and perimeter (to evaluate the reactive surface).

Plaque load was defined as percentage of total dentate gyrus area stained for A β 1-42. It was calculated and defined by (sum plaque area/ sum dentate gyrus area) x 100. The sums were taken over all slides and a singular value for plaque load (percentage) was calculated for each

animal. The number of plaques was normalized to sampled area (n/mm^2). Size distribution was not evaluated. The perimeter was also normalized to sampled area.

To evaluate the number of microglia a different approach was taken, namely the optical dissector method, in which each section is analyzed in a systematically random manner. At 4x magnification, the dentate gyrus was selected as described above (5 sections per animal). But since not the total area was taken for sampling, points were thrown randomly but systematically over the selected area using CAST software (x and y parameters 4, 4, 4, 4), with each point being appointed a constant area of $13,926.4 \mu\text{m}^2$. All points in the area were counted and then used to calculate the sample area.

Microglial cells were counted at 40x magnification. The counting frame was 80%, giving a dissector area of $28,521.3 \mu\text{m}^2$. Meander sampling or the percentage of total area being sampled was 50% of dentate gyrus. The dissector height was $20 \mu\text{m}$, and $15 \mu\text{m}$ corrected. Using the formula below, the total number of cells in the dentate gyrus was calculated. Cells that did not stain to satisfaction or were recognized as not being integer were not taken into consideration, and the typical morphology of microglia was a criterion as well.

$$(1) c_T = (c_C \times a \times p) / d$$

$$(2) a = (A(p) \times z_T) / (A(d) \times z_d)$$

c_T .. total cell count

c_C .. cells counted in sample area

a.. constant

p.. number of points in sample area

d.. number of dissectors

$A(p)$.. area assigned to point

$A(d)$.. area assigned to dissector

z_T .. dissector height (section thickness after cutting)

z_d .. real dissector height (after immuno-staining treatment)

The calculated value c_T gives an approximation of the size of the microglial population in the dentate gyrus.

In order to count microglia normalized to plaque area ("plaque occupancy", which will be defined in the results chapter under 7.), in hypoxia and in normoxia, plaques in a sample area were selected in a systematically randomized manner, and microglia around them counted as in the example described above (Fig. MM05A). The plaque size was also analysed as described above (Fig. MM05B- D). These two values obtained were then pooled for each group and analyzed, normalizing the number of microglia to plaque size.

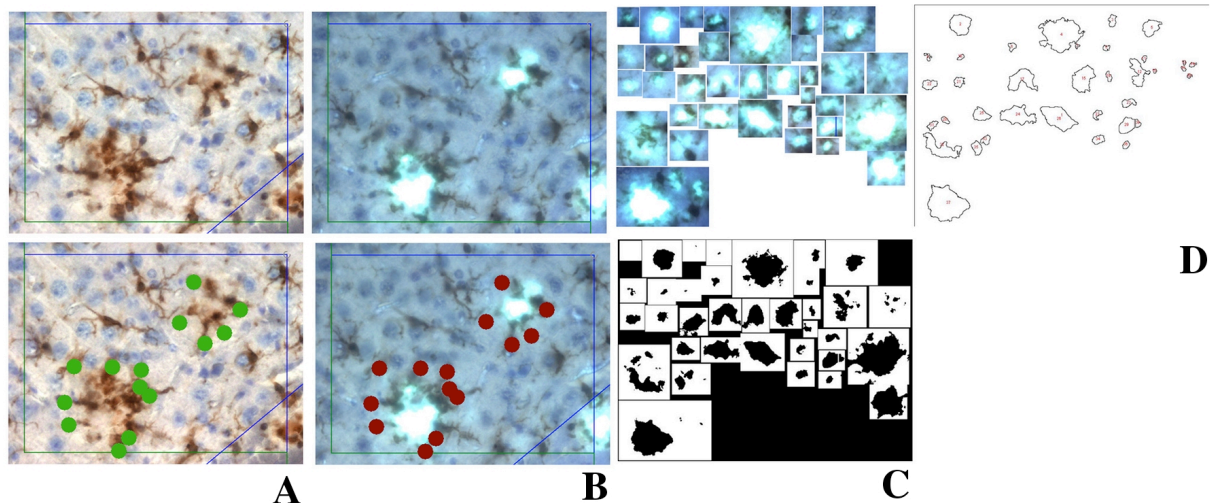


Fig. MM05: Assessment of the number of microglia around A β - plaques. (A) Groups of microglia in the sample space are selected randomly. The number of microglia around a plaque (B) is determined (green/ red dots). Using ImageJ software plaques are analyzed in number and size, by first creating a black mask (C) and then analysing the plaques employing it (D) in number and size.

15. Statistics

Data were expressed as mean \pm SD. Comparison between two groups was carried out by t-test (two-tailed), comparison between several groups was done using one-way ANOVA followed by Tukey's post hoc multiple comparisons test. The confidence interval was set to be 95%. Analysis software SPSS and SigmaStat were employed.

16. List of materials

Chemicals	Ref. No.	Company
Acrylamide (40%)/ Bis solution 29:1 (3.3%C)	1610146	BIORAD
APS		AMERSHAM BIOSCIENCES
Beta Amyloid peptide	SP-BA42-1	INNOVAGEN
BSA	A8022	SIGMA
DMSO	D2650	SIGMA
F12:DMEM 50:50, sterile	21331	GIBCO, INVITROGEN
FBS	SH30070.03	HYCLONE
Gentamycine solution 10 mg/mL	G1272	SIGMA
Glycerol		SIGMA
Guanidine hydrochloride (CH ₅ N ₃ .ClH)	G4505	SIGMA
HCl (37% conc.)		SIGMA
HFLP	105228	SIGMA
L- glutamine	M11-004	GIBCO, INVITROGEN
Lipopolysaccharides (LPS) from E. coli 026:B6	L2654	SIGMA
Methanol		SIGMA
Non-essential aminoacids	M11-003	PAA
Parafin 6060	11609	INSTRUMENTACIÓN TÉCNICO ANALÍTICA S.L.
PBS, sterile	10010	GIBCO, INVITROGEN
Penicilline/ streptomycine solutions		INVITROGEN
PFA		SIGMA
Poly-D-lysine hydrobromide	P6407	SIGMA
TEMED	35925	SERVA
Thiobarbital (sodium thiopental)		BRAUN
Tricine		SIGMA
Tris Base		SERVA
Trizol reagent	15596-026	INVITROGEN
trypsin 0.25%+EDTA	25200-056	GIBCO, INVITROGEN
TWEEN 20	P9416	SIGMA
Urea		SERVA
HE stain		
Accustain Harris hematoxylin solution	HHS32	SIGMA
Accustain eosin and solution	HT110216	SIGMA
Nuclear Fast Red Counterstain		
Aluminium sulfate (Al ₂ (SO ₄) ₃ .xH ₂ O) 5% in H ₂ O	368458	SIGMA
Nuclear fast red 0.1% in above solution, boil to dissolve, filter	60700	SIGMA
Other stains and reactives		
DAPI		SIGMA
Thioflavine- S		SIGMA
Triton X-100 solution	93443	SIGMA
Ethanol		SIGMA
Hydrogen peroxide 30%	95313	SIGMA
Prussian stain		
HCl 37% conc. 1:5 in H ₂ O		SIGMA
Potassium ferrocyanide, Trihydrate (K ₄ Fe(CN) ₆ .3H ₂ O), 10% in H ₂ O	P-3289	SIGMA

Mix above 50:50		
Silver stain		
Processor Plus portioning device		GE HEALTHCARE
Silver staining kit, Protein, "Plus One"	17115001	GE HEALTHCARE
Antibodies		
A11 (1:1000, polyclonal, rabbit anti- mouse)	AHB0052	INVITROGEN
A β 1-42 (1:100, polyclonal, rabbit anti- mouse)	171609	CALBIOCHEM
A β 6e10 (1:1000, monoclonal, anti- mouse, IgG)	SIG39399	SIGNET, COVANCE
Alexa Fluor 568 (1:500, red, goat anti-rabbit)	A11036	MOLECULAR PROBES
Alexa Fluor 488 (1:500, green, donkey anti-mouse)	A11055	MOLECULAR PROBES
GFAP (1:200, monoclonal, anti- mouse, IgG)	3670	CELL SIGNALLING
Iba1 (1:500, polyclonal, rabbit anti- mouse)	1919741	WAKO
Primer		
APP		
5'- CTT GTA AGT TGG ATT CTC ATA TCC G- 3' (forward)	specific	INVITROGEN
5'- GAC TGA CCA CTC GAC CAG GTT CTG- 3' (reverse)	specific	INVITROGEN
stored at -20°C		
Devices/ Tools		
Detection system Western Blot	RPN2132	GE HEALTHCARE
Electrophoresis power supply EPS 601		GE HEALTHCARE
Image Quant		AMERSHAM BIOSCIENCES
Mini Protean system		BIORAD
Multiscan Spectrum luminometer/ spectrophotometer		THERMO ELECTRON CORP.
Nanodrop 2000		THERMO SCIENTIFIC
Noria rotator		SELECTA
Power- Pac 300 electrophoresis power supply		BIORAD
Thermomixer comfort		EPPENDORF
Transfer platform WB		SIGMA
Typhoon 9400 variable mode imager		AMERSHAM BIOSCIENCES
Typhoon Blue Laser Module		AMERSHAM BIOSCIENCES
CAST System		
Mounted PRIOR platform PROSCAN II		PRIOR
Olympus BX61		OLYMPUS
Olympus DP70 camera		OLYMPUS
Software package		OLYMPUS
Cell culture related		
Cell strainer 40 μ m	352340	BD FALCON
Gas mixer "q"		RUSKINN TECHNOLOGY
Hypoxic chamber INVIVO2 300		RUSKINN TECHNOLOGY
Incubator Series II Water Jacketed CO ₂ Incubator		THERMO FISHER SCIENTIFIC
Microscope CKX41		OLYMPUS
Microwave		LG
Waterbath		SELECTA
Working platform TWO30		FASTER

Working platform BIO48		FASTER
Centrifuges		
Centrifuge 5415R		EPPENDORF
Centrifuge 5415D		EPPENDORF
Centrifuge 5810R		EPPENDORF
Centrifuge GS-15R		BECKMAN
SPEEDVAC GYROVAP L		HOWE
Hypoxia- related		
Combustion test kit		BACHARACH
Gas guard		THERMO ELECTRON CORP.
Hypoxic chamber		COY LABORATORY PRODUCTS
Oxygen controller		COY LABORATORY PRODUCTS
Slicing		
Inclusion automat (parafin) ASP300S		LEICA
Microtome RM2125RT		LEICA
Surgery related		
HCT centrifuge "Centrolit II"		SELECTA
KL1500 LCD light		OLYMPUS
Microscope SZX16		OLYMPUS
Consumer articles		
Amersham Hybond-P PVDF transfer membrane	RPN303F	GE HEALTHCARE
Culture plates, plastic, various	NUNC	THERMO FISHER SCIENTIFIC
Filter unit "Stericup"		MILLIPORE
Gloves		NATURFLEX
Hybond Blotting Paper	RPN6101M	AMERSHAM BIOSCIENCES
Hybond-ECL nitrocellulose membrane	RPN2020D	AMERSHAM BIOSCIENCES
Low profile microtome blades LEICA 819		LEICA
Micro tube 1.5 mL	72690	SARSTEDT
Mounting slides "REAL capillary gap microscope slides"	S2024	DAKO
MultiGuard barrier tips (with filter)	35230	SORENSEN, BIOSCIENCE
Pipettes "pipetman"		GILSON
Pipettes, glass		GILSON
Pipettes		EPPENDORF
Pipettes, sterile, serologic, plastic		BD FALCON
RNAse free PCR micro tubes 0.2-1.5 mL		AXYGEN
Syringe micro-fine U-100 insulin 0.3 mL	320838	BD
Surgey instruments		SURGICAL123
15/50 mL PP- Test tubes, sterile	227261	GREINER BIO-ONE
Kits		
AEC+Substrate	K3469	DAKO
DAKO EnVision+System-HRP (DAB) for mouse primary antibodies	K4007	DAKO
DAKO EnVision+System-HRP (DAB) for rabbit primary antibodies	K4011	DAKO
DAKO Faramount Aqueous Mounting Medium	S3025	DAKO
DAKO Fluorescent Mounting Medium	S3023	DAKO
ELISA human beta- amyloid 1-42 kit	KHB3441	INVITROGEN

RC-DC protein quantification kit (method after Lowry)		BIORAD
XTT kit		ROCHE
Software		
CAST software package		OLYMPUS
Image J		NIH
Oligo 6		MOLECULAR BIOLOGY INSIGHTS
Origin 7.0		ORIGINLAB CORPORATION
SPSS		IBM
SigmaStat		STATCON
Animals		
Tg(APP ^{swe} , PSEN1 ^{dE}) mice		JACKSON LABORATORY
Other solutions		
supplement		

Results

1. Working hypothesis

Clinical findings have linked multiple pathologies to AD, as has been described in the introduction. Coexistence worsens dementia, the clinical hallmark of the disease, as compared to pure AD. One general common denominator of these associated pathologies, such as stroke, is the presence of hypoxic tissue conditions. The question was asked, whether there exists a mutual, causal interaction between hypoxia and AD pathology, that could explain the clinical observations. Alternatively, the worsened clinical state of multiple brain pathologies could "simply" be the consequence of multimorbidity, i.e. accumulated disease load, without any causal interaction between the constituents.

2. Physiologic response under the influence of hypoxia

First it was examined whether the transgenic (tg) animals responded to hypoxia in the same way that control (c), i.e. wild- type (wt) littermates do. To our knowledge, this has not been evaluated before.

Animals at the ages of 8 and 14 months (mo) were subjected to hypoxic treatment with 8% oxygen (hypoxia, Hx) or 21% normoxia (Nx) for 20 days. Sample size was 3 for the 8 month age group and 4 for the 14 month group, each for Hx and Nx as well as transgenic and control littermates, respectively, giving a total of 28 animals. The animal age corresponds to juvenile and old age, as the mean age of mice is around two years. The plaque desposition onset of the transgenic animal model lies at about 6 months, so by choosing 8 and 14 month old animals, it was possible to evaluate amyloid deposition at an early stage, as well as in a progressed state. Treatment of older animals or longer periods of hypoxia resulted in a high mortality (data not shown). All animals were fed and exposed to the same constant light and dark cycles.

Behavioural observations were difficult to standardize, as the hypoxic treatment occurred in a sealed chamber. Testing would have included stopping the exposure temporarily. As this was not deemed acceptable under the working hypothesis, behavioural testing was not performed. However, as assessed by mere observation, animals under hypoxia tended to move very little, as the treatment posed a significant challenge to their fitness. They were not observed to be more aggressive or otherwise presenting altered behaviour, compared to the control littermates under normoxia.

Neuronal damage was not assessed, as our primary marker of causal interaction between hypoxia and AD was A β - protein deposition. It is likely, that neuronal damage is more prominent in animals subject to hypoxia, both within the transgenic and the control group. However, this was not a focus of the experiments.

Two markers were chosen to evaluate the adaption to the hypoxic stimulus: First, hematocrit (HCT), which is defined as the percental volume of cellular elements in the blood. In principle, hypoxia stimulates erythropoiesis, increasing oxygen transport capacities of the blood through increased cell number and percentage. Second, weight loss was recorded as difference between weight at the beginning and the end of the treatment.

Comparing HCT within the age groups per treatment, there was no significant difference observed between transgenic animals and control littermates (Tab. 1, $p > 0.05$, One Way ANOVA/ Tukey for all groups, $p > 0.05$, Student's T- test for age/ treatment group, e.g. 8 mo/ Hx/ tg vs. 8 mo/ Hx/ c) (Fig. R01).

age	treatment	genotype	mean	S.E.M.
8 mo	Nx	tg	0.45	0.08
		wt	0.40	0.11
	Hx	tg	0.90	0.04
		wt	0.84	0.04
14 mo	Nx	tg	0.50	0.03
		wt	0.50	0.04
	Hx	tg	0.86	0.07
		wt	0.86	0.12

Tab. R01: HCT values of the experimental groups.

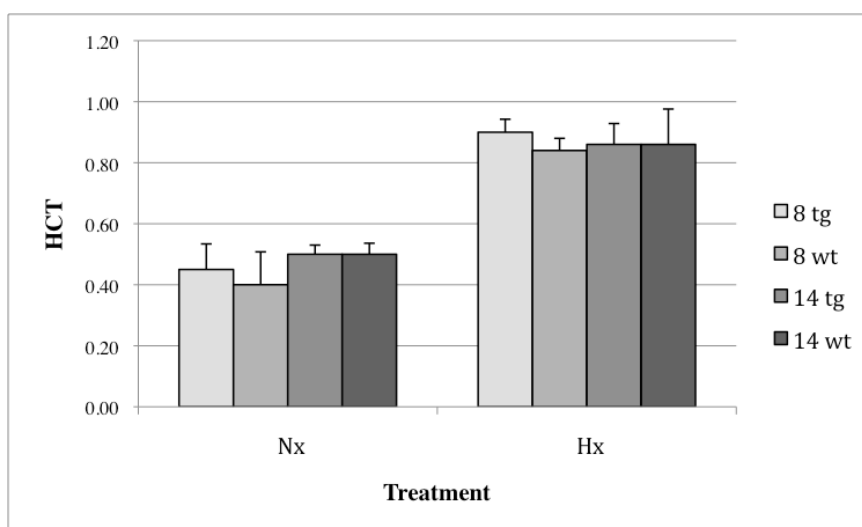


Fig. R01: HCT increases as response to the hypoxic stimulus in animals of all ages.

Animals exposed to hypoxia showed an increased HCT, indicating increased erythrocyte production to secure oxygen supply throughout the body (transgenic and control animals of all ages pooled; 0.86 ± 0.07 for hypoxic conditions as compared to 0.46 ± 0.07 for controls, $p < 0.0001$, Student's T-test) (Fig. R02).

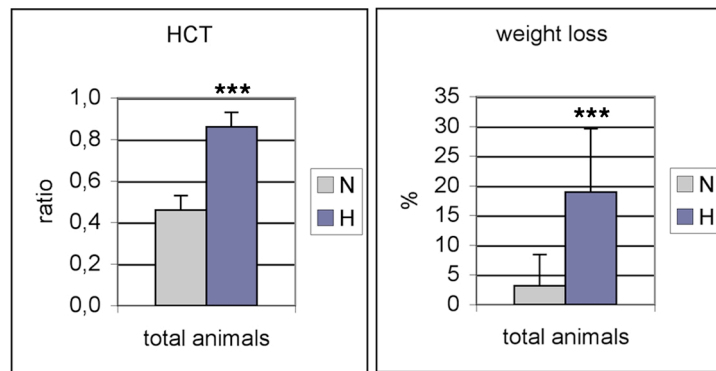


Fig. R02: Pooled HCT and weight loss, normoxia vs. hypoxia. HCT is elevated in animals under hypoxia (H), as is weight loss (normoxia, N) ($p < 0.0001$, Student's T-test).

The weight loss in percent of the weight at the start of the treatment, although highly variable between samples within each group, confirms that hypoxic treatment puts significant stress on the animals (18.9 ± 10.7 % in Hx compared to 3.2 ± 5.3 % in Nx, $p < 0.0001$, Student's T-test) (Fig. R01 and R02).

Summarizing these findings, hypoxia has a measurable effect on the treated group, and transgenic and control animals do not differ in their response as far as the chosen parameters are concerned.

3. Histology confirms the effect of the hypoxic treatment

Changes under Hx also occur within the structure of the brain. Most importantly, new vessel formation is triggered through an increased shedding of VEGF by vascular endothelial cells, amongst others (see introductory chapter). Histologic sections were prepared to evaluate this process known as reactive angiogenesis and to evaluate other potential tissue characteristics such as cerebral infarctions. The latter are known to correlate with increased blood viscosity, i.e. HCT. Furthermore, the question was raised, whether the modified hemodynamics could cause hemorrhages. To discard this possibility, brain slices were randomly chosen from both groups of different positions in the brain. These were stained with Prussian blue, also known as Berlin blue stain, a method that marks free iron ($\text{Fe}^{2/3+}$) through a bright blue colour. This iron becomes liberated when erythrocytes lose their integrity through extravasation or in the clotting process (Fig. R03-05).

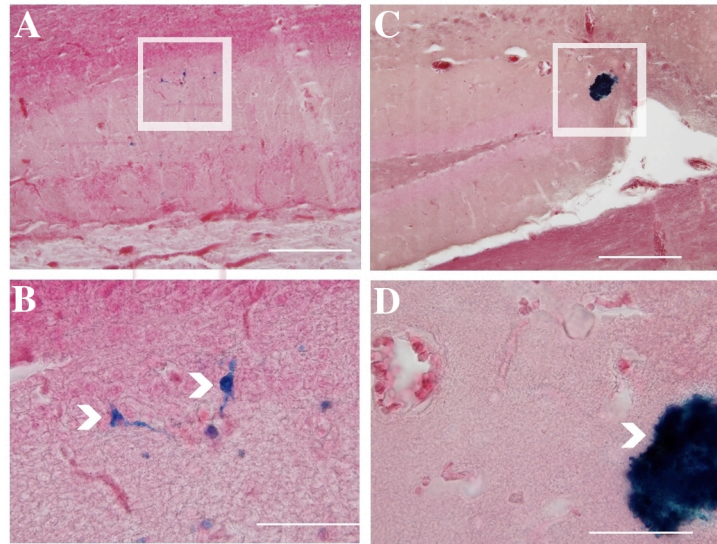


Fig. R03: Histology of an 8 month old, wild- type animal under hypoxia. On the left, cells are marked blue as a sign that they contain free iron (arrows in B). In the hippocampus, a vessel is occluded, possibly because of altered hemodynamics under hypoxia (arrow in D). Prussian blue stain. Scale is 50 and 200 μm respectively.

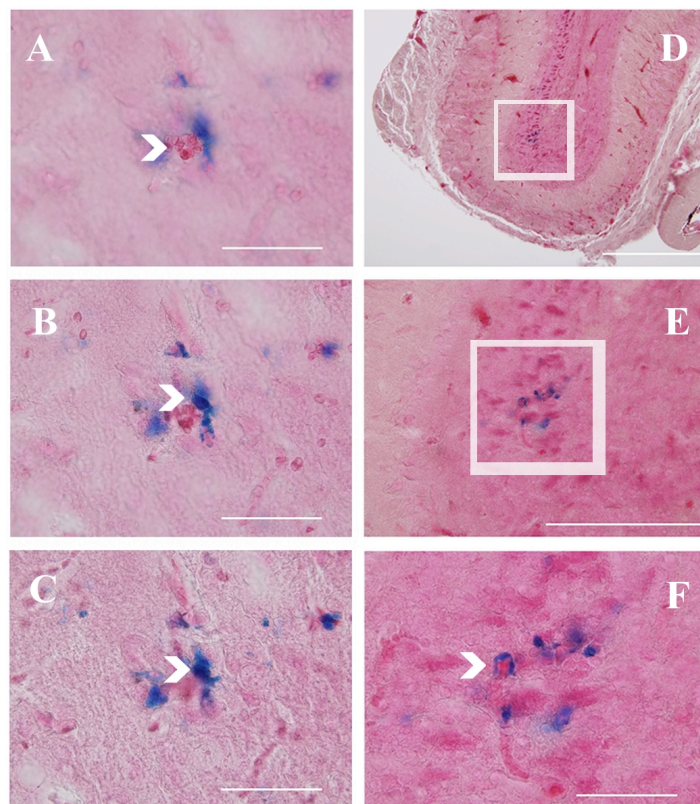


Fig. R04: (A-C) Stained cells surrounding a vessel (arrow in A), at variable levels of the z- axis, to illustrate the cellular character of the stained structures (arrows in B, C and F). From the staining, only small areas are affected (D, marked is a portion of the olfactory bulb), with stained cells surrounding vessels and lying in groups of only several cells (E, F with arrow). Scale is 200 (D), 150 (E) and 50 (A-C, F) μm . Prussian blue stain.

Angiogenesis was very prominent in the animals under Hx throughout the brain. It was especially developed in the vasculature within the cortex and surrounding the hippocampus (Fig. R05).

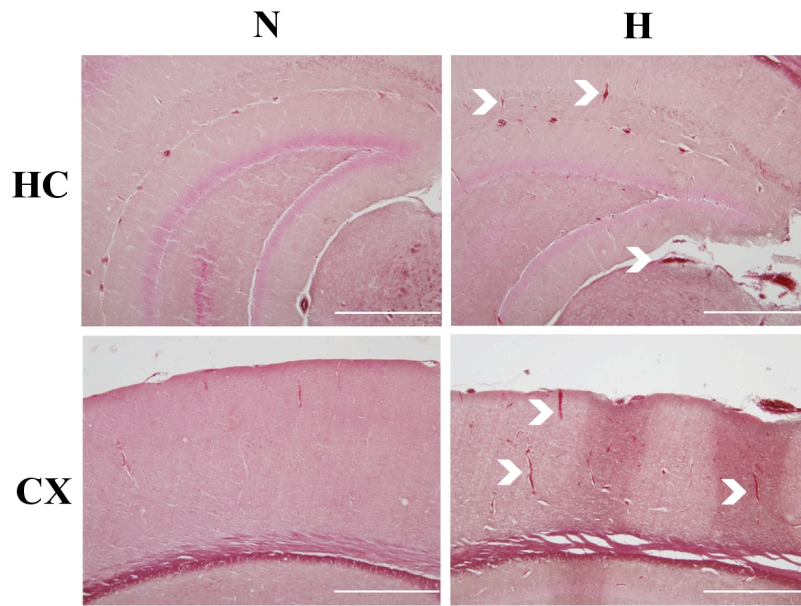


Fig. R05: Physiologic response to a hypoxic stimulus. Prominent reactive angiogenesis (arrows) in the cortex (CX) and in the hippocampal formation (gyrus dentatus, HC) under hypoxia (H) but not under normoxia (N). Prussian blue stain. Scale is 500 μ m.

Small stained areas were found across 8 and 14 month- old animals, wild- type and transgenic, under hypoxic treatment in the sections sampled, without any quantitative difference between them, as was assessed by observation (data not shown) (Fig. R03-05). The regular behaviour of the animals in all groups, including the ones treated with normoxia, confirms this as a minor finding. Major clotting or hemorrhages would result in clinical impairment and behavioural change. Minor alterations included clotting of small vessels (Fig. R03). Blue stained cells were also found present (Fig. R03, R04A-C). They most likely correspond to the macrophages/ microglia lineage as this cell type is able to internalise free iron- containing blood particles through phagocytosis. This blood might have leaked from vessels that lost their integrity through clotting. The fact that blue stained cells were found only in groups and only surrounding vessels supports this interpretation of the findings (Fig. R04). Double- labelling studies would be necessary to assess whether these cells are in fact microglia. Further identification of this cell population was not carried out, because no information was to be gained from this which would have helped our working hypothesis.

4. Plaque load is not significantly affected by hypoxic treatment

Now it was asked whether hypoxia could change the A β - protein quantity in the brain. This was assessed in two ways: First histologically, by staining for A β - protein depositions, known as plaques and second quantitatively, as plaque load. The antibody used only stains solid and not diffuse plaques (Fig. R06). The latter refers to plaque- like structures of which the exact

boundaries are hard to assess due to their diffuse nature and pattern. However, the exact distinction between diffuse and solid plaques is not well defined. Histologically, diffuse plaques are not easily or reliably quantifiable, which is why it was decided to focus on the solid plaque load in histology. However, histology would only allow to quantify visible structures. To circumvent this restriction, the concentration of A β 1-42 protein in the brain was measured using an ELISA approach.

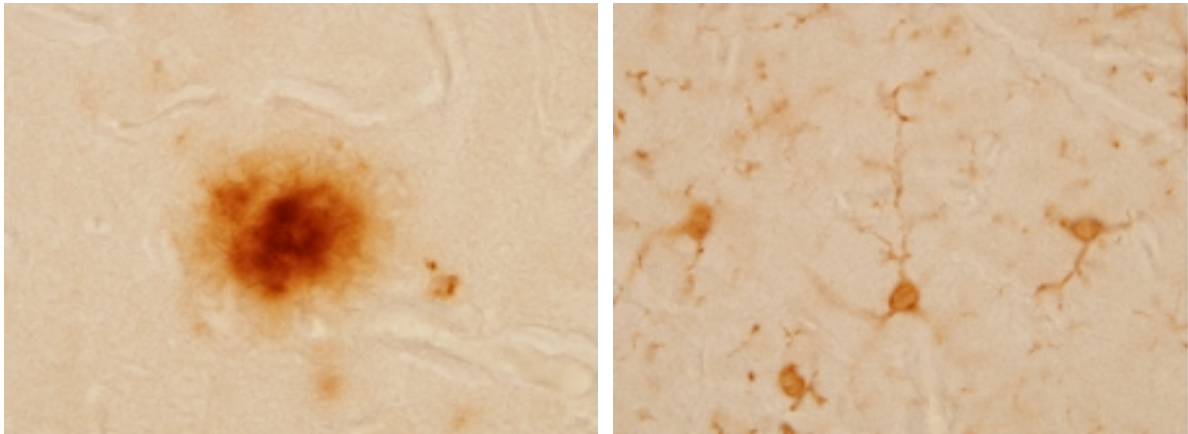


Fig. R06: Histology of an 8 month- old, transgenic animal under normoxia. A β - plaque (left) stained with anti-A β 1-42, which marks only solid plaques. Microglial cells (right) presenting an unstimulated phenotype with the "arm's length" spacial distance between each two cells.

Brain slices for histologic quantification were chosen in the following manner: After fixation and having been sectioned at 20 μ m coronarily, sections were screened as to where the hippocampus first reaches the ventral brain surface. In addition, two sections before and after this point were also chosen, with an inter- sectional distance of 260 μ m. Sections from hereon were quantitatively assessed by projection onto a computer screen, where image manipulation was feasible. If there was any doubt about a given structure, the image was directly assessed through the microscope.

In each of the selected sections, a part of the hippocampal formation known as the dentate gyrus was delineated with a corresponding selection tool (CAST statistical quantification software package). This anatomical structure was chosen on the grounds that it is easily and reproducibly identifiable within all sections of interest and that it has a reasonable size for quantification. Furthermore, as a part of the hippocampus, it is one of the areas known to be affected most by AD. The distribution of deposited plaques within this anatomical structure is not homogeneous, so a total of 100 % of the area selected had to be quantitatively assessed by plaque count, in order to obtain reliable results with acceptable deviations for the same sample being quantified (data not shown). The CAST software provides an algorithm, which

assures, that multiple image details (high magnification) represent 50% of the structure of interest (delineated with a low magnification). Again, the size of the dentate gyrus was crucial to keep the time spent on each quantified section within reasonable boundaries. The image details were photographed, summing up to and covering 50% of the area of interest, i.e. the dentate gyrus.

Because it would not have been feasible to count the number of A β - plaques manually in such a large area, the Image J image analysis software was employed for quantification. Interest lied in two parameters: the total number of A β - plaques, and the area in percent that these depositions represent within the whole area of interest. The reasoning behind the latter is that it allows an estimation of average plaque size when the total number of plaques is taken into account. For example, if the total number of plaques has the same value for two groups, but in one group, the area that those plaques represent (in %) is bigger, then it can be argued, that the average plaque must also be of a larger size.

Visually, no difference was observed between groups under hypoxia and normoxia, as illustrated by Fig. R07. What can be seen is that the plaque deposition between 8 and 14 months of age is very progressive, which is especially true for the delineated anatomical structure of the dentate gyrus.

To our surprise, no significant differences in A β - protein load were found: Comparing the number of plaques in 8- month old animals under hypoxic conditions with those of their control littermates, did not reveal significant differences ($35.2 \pm 9.9/ \text{mm}^2$ in Hx against $29.3 \pm 4.2/ \text{mm}^2$ in Nx, $p > 0.05$, One Way ANOVA/ Tukey). Since the total number of plaques was not altered by hypoxia, it was asked, whether the mean size of the β - amyloid (A β) depositions was modified. For this the percentage plaque area was determined, as has been explained above. Similar to the total number of plaques, no significant difference in the area of A β - protein depositions was found ($0.90 \pm 0.20 \%$ in Hx against $0.91 \pm 0.25 \%$, $p > 0.05$, One Way ANOVA/ Tukey). It can thus be argued, that neither the total number of plaques, nor their mean size changes under hypoxic treatment in 8- month old (transgenic) animals (Fig. R08A, B).

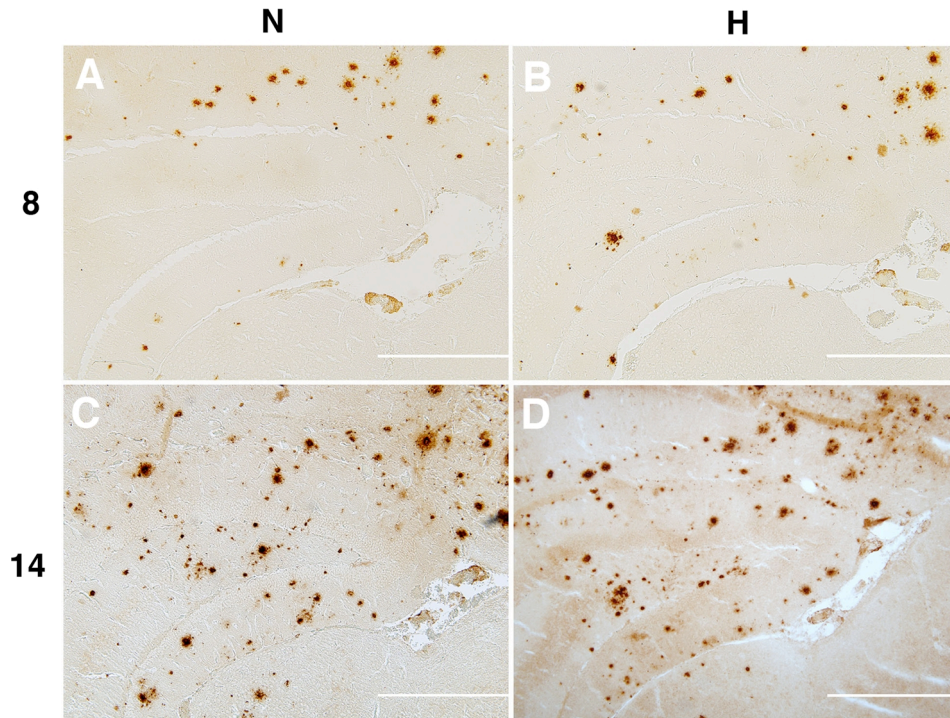


Fig. R07: (A-D) No altered amyloid deposition under hypoxic treatment in the hippocampal dentate gyrus. Visually, no difference in plaque deposition between Nx and Hx can be observed in either age group. Sections stained with antibody against A β 1-42, scale 500 μ m, N: normoxia, H: hypoxia, numbers indicate age [mo].

Surprisingly, for 14-month old animals, the same holds true: No significant alteration in number (74.8 ± 7.4 in Hx compared to 61.1 ± 4.6 in Nx, $p > 0.05$, One Way ANOVA/ Tukey) or percentage plaque area (1.72 ± 0.27 % in Hx against 1.48 ± 0.27 % in Nx, $p > 0.05$, One Way ANOVA/ Tukey) was detected (Fig. R08A, B).

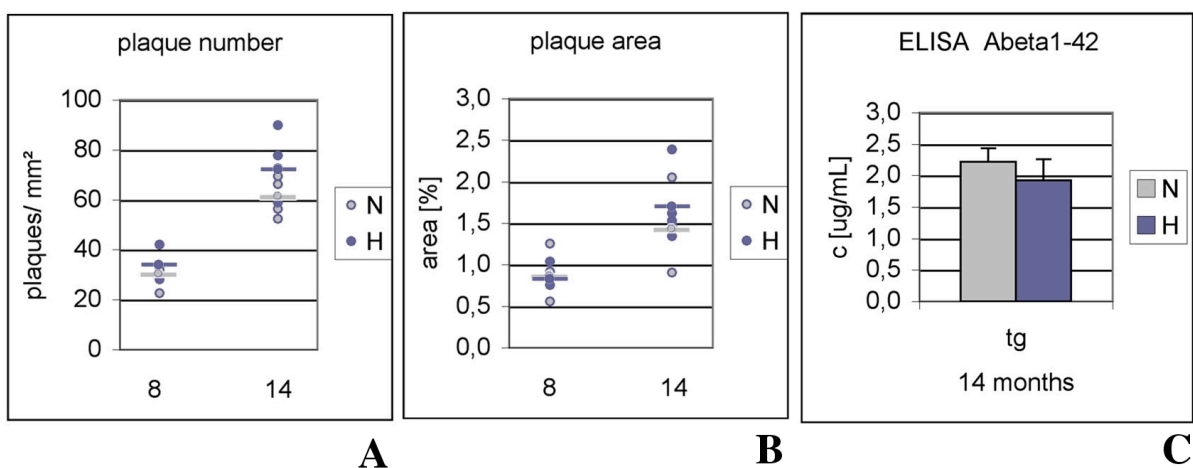


Fig. R08: Histology shows that neither the total number of A β - plaques (A) nor the occupied area (B) (and by extension their mean size) differs between N and H groups of either age group. Bars indicate mean values, dots individual ones. (C) ELISA reveals equal A β - protein loads for normoxia (N) and hypoxia (H) treated animals of 14 months.

To confirm this observation, the A β 1-42 peptide was quantified, i.e. the exact same protein that had been marked histologically, employing an ELISA. Animals of 8 months of age presented similar amyloid loads ($0.41 \pm 0.11 \mu\text{g/mL}$ under Hx against $0.47 \pm 0.08 \mu\text{g/mL}$ under Nx) as did 14- month old animals ($1.93 \pm 0.33 \mu\text{g/mL}$ under Hx compared with $2.22 \pm 0.21 \mu\text{g/mL}$ under Nx). No significant difference in A β 1-42 load was found within the age groups ($p > 0.05$, One Way ANOVA/ Tukey), confirming the histologic observations (Fig. R08C).

Summarizing these findings, it can be stated, that hypoxic treatment does not alter the A β 1-42 protein load in the brain, neither in young nor old animals, as assessed both, histologically and by total ELISA quantification of A β 1-42 protein.

5. Oligomer formation under hypoxic treatment

Since hypoxia did not alter the quantity of the A β - protein, it was asked whether it influenced it qualitatively?

As described in the introduction, A β - protein does self- accumulate in various grades of complexity, i.e. as monomer, oligomer or fibril. Since oligomers are known to be the most neurotoxic "species" of the A β - protein, it was hypothesized, that under hypoxic treatment their quantity could increase. This change in the spectrum of the A β - species could, without any change in total A β - protein load, lead to increased neurotoxicity in animals under hypoxia.

An antibody that recognizes various forms of oligomers, amongst them the A β - oligomer, was employed. Although somewhat unspecific, this is in our view the best method to assess oligomer quantity. The problem with methods such as classical SDS- PAGE and subsequent Western blotting is that the protein conformation is not kept intact but rather denaturated throughout the process. But an intact conformation is essential in order to evaluate aggregated A β - protein monomers, i.e. oligomers.

Initially a dot- blot was employed, leaving the protein conformation intact and in its original state. The question was whether hypoxia could enhance oligomer formation. It was possible to visualize that there is a quantitative increase in oligomers under hypoxia (Fig. R09A). Since the sample size in this initial experiment was two in each group, statistics could not be applied.

A try to reproduce these results in a native PAGE and subsequent Western blot was undertaken, employing a gel concentration of 16% to capture A β - monomers, which have a low molecular weight (4.7 kDa). Again, this methodology left the native conformation of

aggregated monomers, i.e. oligomers, intact. It was found that the amount of oligomers seems to increase under hypoxia (Fig. R09B).

Future research is necessary to assess these preliminary findings more thoroughly. However, there is a trend towards enhanced oligomer formation under hypoxia.

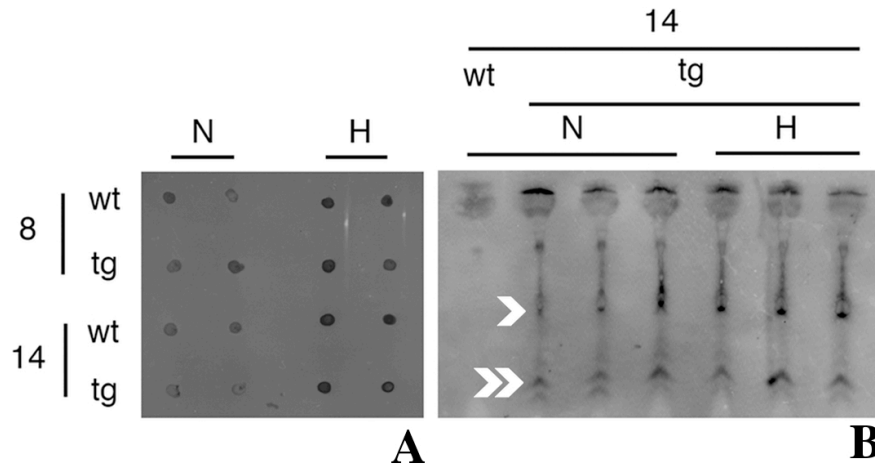


Fig. R09: (A) Dot blot with the oligomer antibody (A11), which (amongst others) marks A β - oligomers. Apparently, animals under normoxia (N) have lower quantities than their littermates under hypoxia (H). (B) Native Western blot with anti- A β 1-42 antibody (6E10). At the bottom the monomer (4.7 kDa, double arrow) is marked, with the next band towards the top weighing around 12kDa (three- monomer- aggregates, single arrow) and classifying as oligomer. A trend could be suggested, with hypoxia increasing the oligomer quantity. Interestingly, two monomers do not aggregate.

6. Microglia under hypoxic conditions

It was asked, whether hypoxia alters the cellular response to the protein. Microglial cells have been described as the first cells to encounter the A β - protein "threat" in the shape of plaques, i.e. A β - protein aggregates. They then try to encapsulate and subsequently degrade them (see introduction, 4.), which is illustrated in Fig. R10. Therefore, attention was placed on this population.

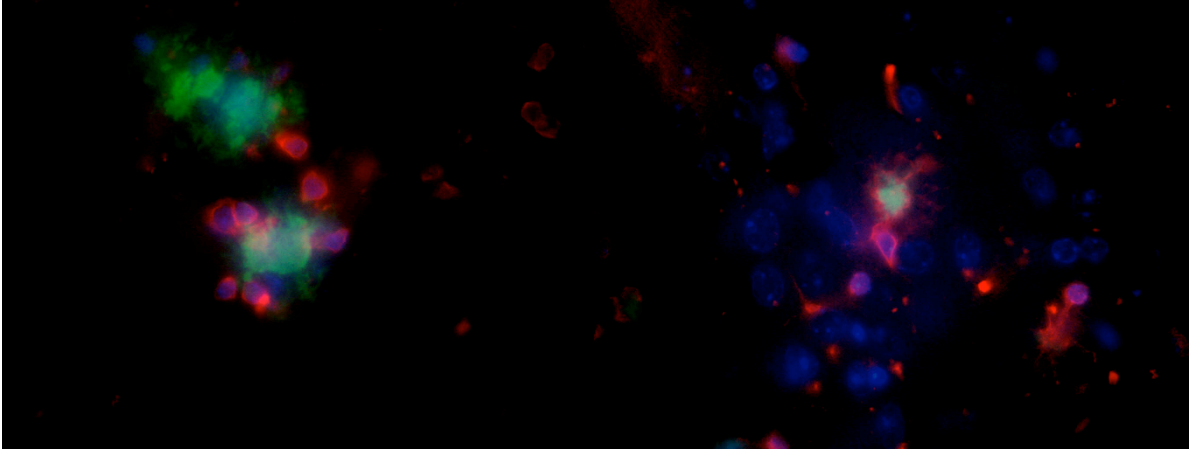


Fig. R10: Microglial cells encountering A β - plaques. In the left image, multiple Iba- positive, microglia cells surround a plaque. In the right image, one Iba- positive cell internalizes a plaque. In general, microglia move towards plaques to limit their expansion and degrade A β - protein. Microglial cells (red, anti- Iba1), plaques (green, Thioflavin-S stain), nuclei counter stain (blue, DAPI).

Again, 8 and 14 month- old animals were selected for the experiments. Sections were selected qualitatively and quantitatively as described under 14. in the materials and methods chapter. In short, 50% of the area (hippocampal dentate gyrus) was randomly selected, the cell number quantified using the CAST software with its cell counting tools. The reduction in the sampled area compared to the plaque- quantification (100%) was feasible, because microglia are much more homogeneously spread across the dentate gyrus. The microglial cell lineage was marked using an antibody against Iba1, a surface co- receptor, which in the brain is exclusively expressed in this cell-type (Fig. R10). The total cell count of microglia in the hippocampal dentate gyrus (hereafter simply referred to as total cell count) was calculated as was described under 14. in the materials and methods chapter.

There are several factors that influence the amount of microglia in the brain tissue, namely genotype, age and hypoxia. First, transgenic animals are observed to have a larger microglial population than their wild- type littermates (Fig. R11 an Tab. R02). This is attributable to the fact, that the former group, through expression of the A β - protein, has an inherent inflammatory stimulus present. This stimulus induces microglial activation, exemplified by Fig. R12, and also leads to larger numbers of microglia present in the brain tissue (compare Fig. R13A to B for 8 month old animals and R13C to D for 14 months).

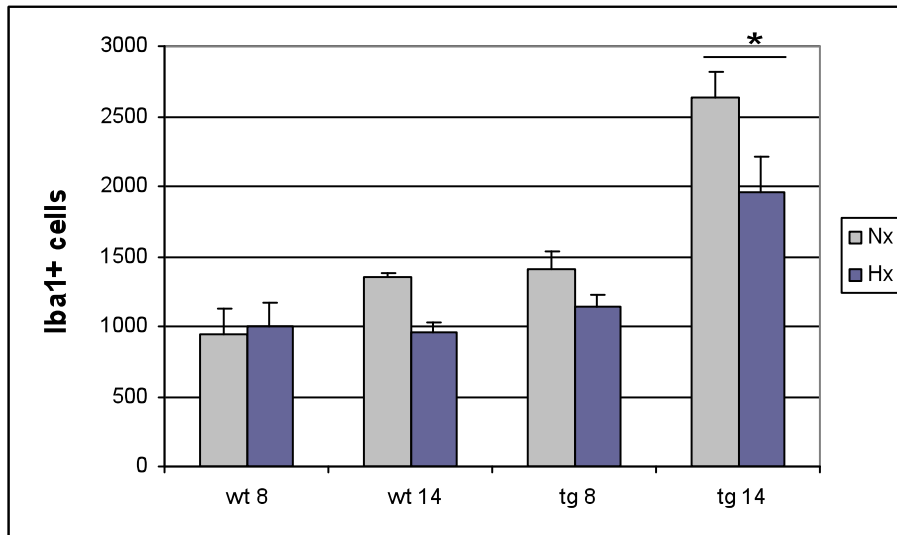


Fig. R11: Total cell count of microglia in the hippocampal dentate gyrus in wild- type (wt) and transgenic (tg) animals under normoxic (Nx) and hypoxic (Hx) treatment. Total, Iba1- positive cells were assessed for the whole hippocampal gyrus dentatus, with a sampled area of 50% of the gyrus area. Note, that in general, transgenic animals, especially at 14 months, present with a higher microglia cell count than their wild- type littermates. Multigroup comparison reveals a significant decrease in the microglia cell count in "tg 14" animals under hypoxia (asterisk indicates a significance of $p < 0.05$, ANOVA/ Tukey). Single group comparison reveals a significant decrease of the microglia cell count for "wt 14" animals under hypoxia ($p < 0.01$, Student's T- test).

age	type	treatment	Iba1+ cells (mean)	S.E.M.
8	wt	Nx	941	183
		Hx	1002	169
	tg	Nx	1409	121
		Hx	1139	92
14	wt	Nx	1359	15
		Hx	962	63
	tg	Nx	2633	178
		Hx	1963	254

Tab. R02: Values from the graph in Fig. R12. Iba1- positive cells are microglia.

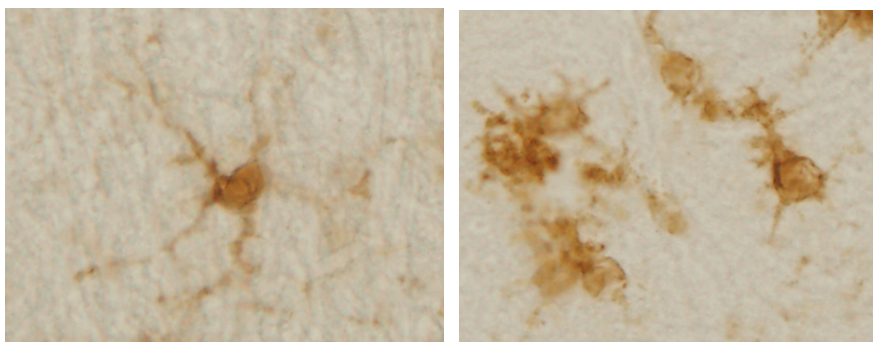


Fig. R12: Activation of microglia leads to a change in phenotype. Images are taken from two animals, one 8 months, wild- type (left) and one 8 months, transgenic (right), both under normoxia. An unactivated, surveilling microglial cell (left) is characterized by long processes and stays at an "arm's length" distance from any neighboring microglial cell. Activated microglia (right) loose their processes and have an increased cytoplasm-nucleus relation. Also, the homogenous positioning in the context of neighboring microglial cells is abandoned, and various cells can be found within a small area (see also Fig. MM01).

Second, the total number of microglia cells increases with age (Fig. R11 and R13). This is especially true for transgenic animals, where the number of microglia nearly doubles in a six month period, i.e. from 8 months to 14 months (compare Fig. R13B to D). However, an increase in microglia is also visible for wild- type animals (compare Fig. R13A to C).

Third, the total number of microglia cells decreases under hypoxia in old animals (Fig. R11, 13 and Tab. R02). Visually this can be assessed by comparing old, hypoxic animals in Fig. R13 (H, 14) to their normoxic controls (N, 14). The image in the latter gives the impression of a more dispersed microglia population, through which the staining appears less intense. When quantified, this difference holds true. Multigroup comparison reveals a significant decrease in the total number of microglia in the gyrus dentatus of old, transgenic animals under hypoxia (Fig. R11, asterisk indicates a significance of $p < 0.05$, ANOVA/ Tukey). None of the other groups reaches significance under a multigroup comparison. However, when observing the graph in Fig. R11, the difference in the number of microglia seems substantial for old, wild- type animals also. This observation reaches significance through a single- group comparison ($p < 0.01$, Student's T- test). However, future reasearch should increase the sample size to gain more statistical certainty.

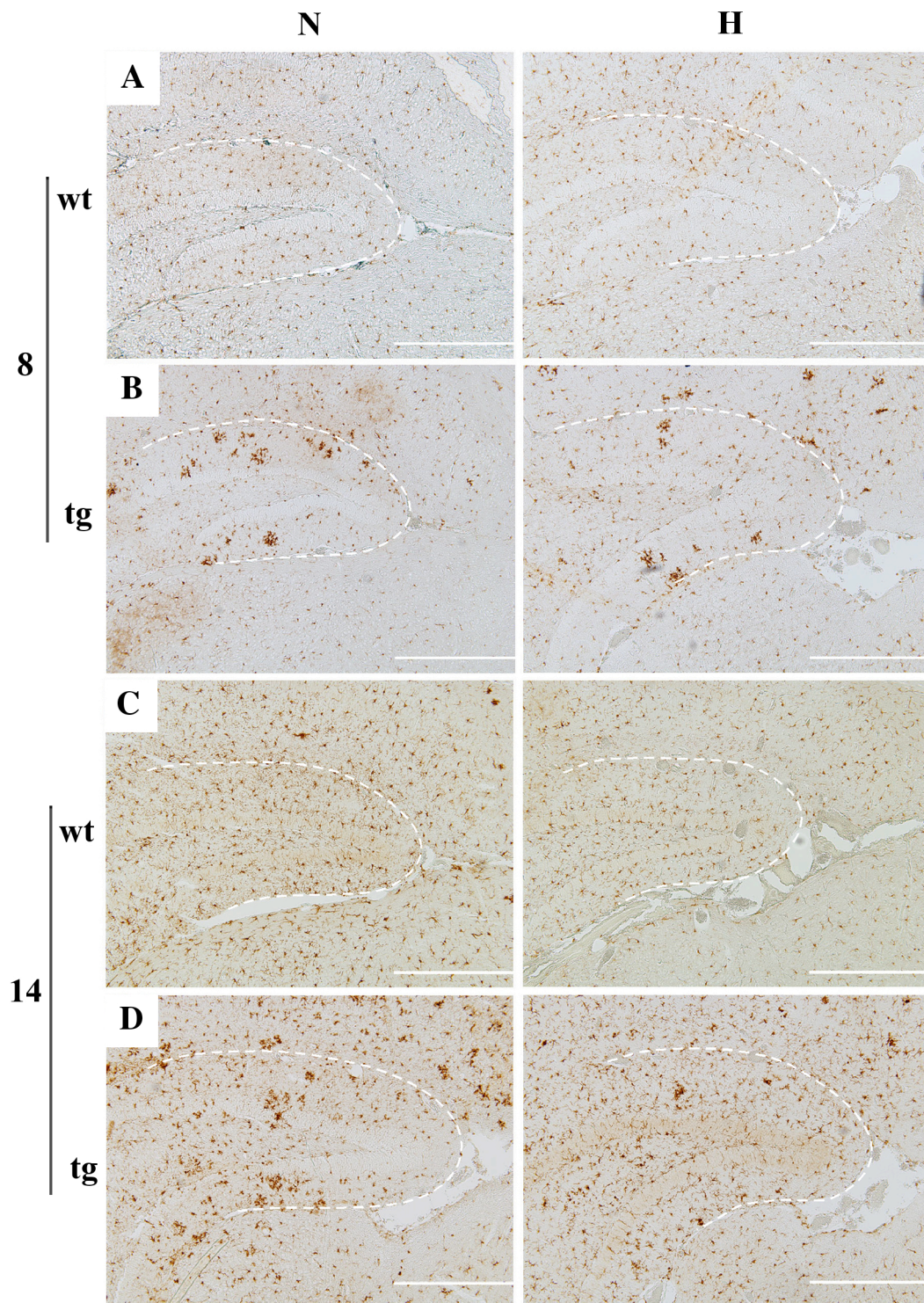


Fig. R13: Microglia in animals of different genotype (transgenic [tg], wild-type [wt]), of different age (8 and 14 months) and under different conditions (normoxia [N], hypoxia [H]). Marked (string line) is the hippocampal dentate gyrus, from which a sample area of 50% was chosen to quantify microglia in (compare graph in Fig. R11 and numbers in Tab. R02). Scale 500 μ m. Paraffin sections stained for Iba1, a microglia marker (brown colour). In tg animals the typical microglia behaviour of grouping around A β - plaques can be observed (arrows).

Summarizing, it can be stated, that the total number of microglia in the hippocampal dentate gyrus, and, it can be argued, by extension the brain, changes dynamically with various factors.

First, transgenic animals present an increase in microglia. Second, microglia increase with age. Third, microglia decrease under hypoxia, but only do so significantly in old animals.

7. Correlation between the number of microglia and vessel density

As microglial cells were found to be diminished in the oxygen- deprived group, it was asked, whether this absence correlated with vessel density. The latter is a constraint on how much oxygen can be transported into a specific region. So it was hypothesized, that the number of microglia per mm² plaque, as had been assessed previously, correlated with the regional vessel density. The reasoning behind this approach is the fact, that microglia are dependent on oxygen, which reaches them through blood vessels and subsequent diffusion through the brain tissue. This raises the following question: Does less oxygen supply as estimated by vessel density correlate with less microglia per mm² plaque?

A triple staining technique was employed, which includes staining for Iba1 (microglia), an unspecific secondary IgG anti- mouse antibody to reveal globulin structures (vessels), and finally super- staining with Thioflavin-S (plaques). The somewhat unorthodox staining of mouse brain vessels was necessary, due to the absence of potent antibodies. However, the staining results were beforehand correlated with a hematoxylin- eosin (HE) stain, and the vessel staining capacities of the unspecific secondary antibody were deemed acceptable for our purpose. As for animal selection, 14 month- old animals of both groups, normoxia and hypoxia, were pooled. This augmented the sampled areas. Furthermore, a distinction according to treatment was not necessary under the question posed. The number of vessels was determined with the help of a randomly- oriented, multi- circular form, included in the CAST software. The number of crosses of vessels with the lines of this form was counted, and taken as the parameter for vessel density. This methodological approach draws on Cavalieri's principle. According to it, two bodies have the same volume, if their cut surfaces, in planes parallel to a ground surface, have the same area.

The number of Iba1 positive cells per 100 μm² plaque area was determined, with the same technique as had been used before. Then, this value was correlated to the number of vessels in the respective plaque's perimeter. As shown in Fig. R14, a positive correlation was found between the number of microglial cells and vessel density. More microglial cells were present when more vessels were found ($R^2 = 0.16$, Pearson Correlation Test, 2 Sides $p = 0.002$).

It can be deduced, that although microglial cells have been shown to be resistant to hypoxic stimuli, they are dependent on adequate oxygen supply in the long run. If this supply does not meet the cells' needs, the capacity to confront Aβ- protein depositions is compromised.

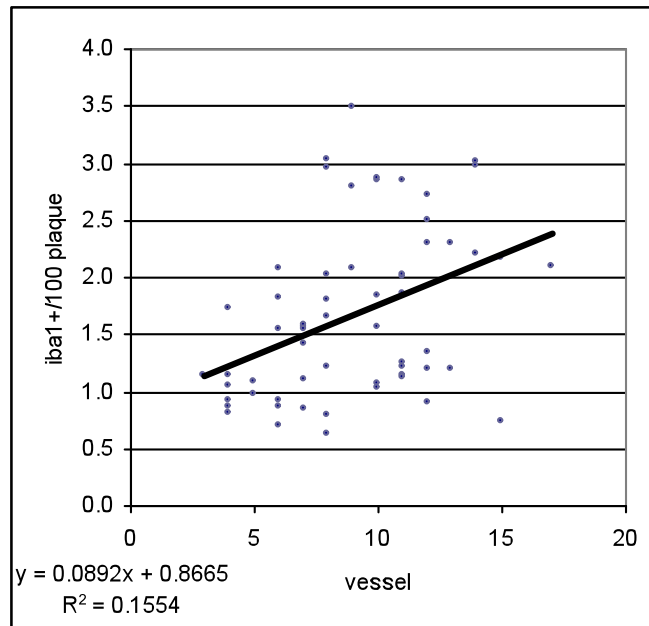


Fig. R14: Correlation between Microglia per plaque with vessel density. Statistics: Pearson- Correlation- Test, 2 Sides, ($p < 0.01$).

8. Cultured microglial cells respond with increased viability to hypoxic stimuli

In order to analyze whether hypoxia influences cell viability of microglia, cell culture experiments were performed with microglia- enriched primary cell cultures.

These cell cultures were exposed to hypoxia and the effect on cell viability evaluated using and XTT assay. Exposition to 1 % oxygen was for 4, 24 and 48 hours. Under 24 and 48 h of hypoxia, cell viability was detected to be significantly increased, compared to cells cultivated under normal oxygen conditions (24h: relative O.D. 1 ± 0.04 in Nx versus 1.25 ± 0.09 in Hx, Student's T-test $p < 0.01$; 48h: relative O.D. 1 ± 0.04 in Nx against 1.35 ± 0.07 in Hx, Student's T-test $p < 0.001$; 3 repetitive experiments respectively, results pooled, then analyzed). However, no significant difference was detected after 4h of exposition to the hypoxic stimulus (relative O.D. 1 ± 0.05 in Nx compared to 0.95 ± 0.05 in Hx, Student's T-test $p = 0.45$) (Fig. R11).

It can be deduced, that the microglial loss does definitely not occur in the short- term, but that it is most likely due to the prolonged exposition to hypoxia. Accordingly, microglial cells must disappear at later stages of exposition to oxygen deprivation.

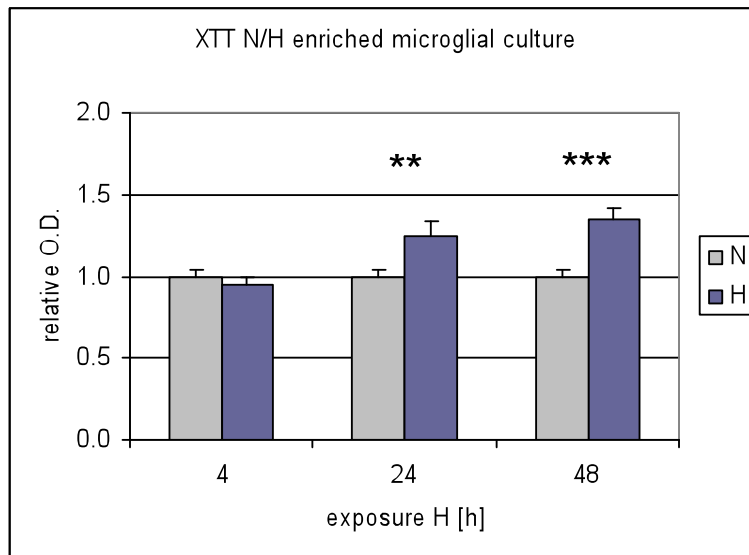


Fig. R15: Microglial cell viability after 4, 24 and 48 hours of hypoxic exposition. Two stars mean $p < 0.01$, three $p < 0.001$. No significant difference after 4 hours, but increased viability of cells under hypoxia compared to normoxia after 24 and 48 hours of exposition.

9. Plaque occupancy under hypoxia

One of the important mechanisms in controlling the A β - protein depositions is the microglial function to surround a plaque, restrict its extension, minimize the plaque's reactive surface, and ultimately attempt to degrade it. With the finding of less microglia under long- term hypoxia, we wondered whether the function of microglia was compromised in the hypoxia group. A significant decrease in the total number of microglia in the hippocampal dentate gyrus due to hypoxia was only found in 14 month- old, transgenic animals. Therefore it was decided to focus only on this group.

A parameter called "plaque occupancy" was coined, to assess the microglia function to confront A β - plaques. Plaque occupancy is defined as the number of microglia in spatial proximity to one square millimeter of A β - plaque. This means, that microglia restricting one plaque are counted, and then normalized to this plaque's area. It was hypothesized that hypoxia would decrease plaque occupancy. This was supported by visual findings as exemplified in Fig. R16.

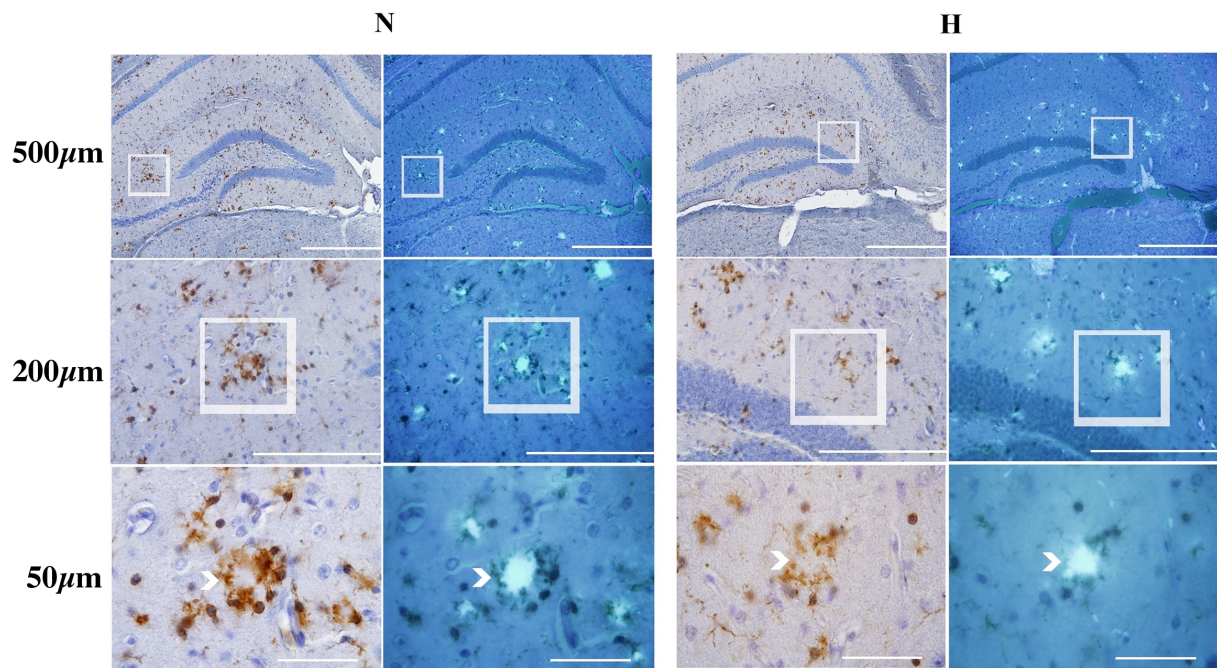


Fig. R16: Detailed view of microglia with the typical accumulation around A β - plaques. Dentate gyrus of 14 months old, transgenic animals. Scale 500, 200 and 50 μ m. Magnifications 100, 200 and 1000, respectively. Less microglia are present under hypoxia (H) than normoxia (N). Triple- stain: Anti- Iba1 and HE counterstain, to show microglia and nuclei under white light (left image of N and H, respectively) and Thioflavin- S stain to show plaques under UV- light (right image of N and H, respectively).

As described under 14. in the materials and methods chapter and illustrated in Fig. MM05, plaque occupancy was assessed in the following way: Randomly chosen plaques from 14 month- old animals were selected, with a representative number of plaques for each animal and in normoxia and hypoxia (in total 176 plaques). Subsequently, the plaque area was determined and the microglia present around the plaque were counted (Fig. MM05A and B), with plaque occupancy being calculated thereafter (Fig. MM05C and D). Then, the obtained values were pooled across animals in the respective groups, namely normoxia and hypoxia.

This quantitative analysis revealed a significant drop in plaque occupancy in old animals under hypoxia (Fig. R17). Under normoxia, 46.24 ± 4.41 (mean \pm S.E.M.) Iba1- positive cells surround 1 mm² of plaque area, but only 20.87 ± 4.27 cells are present under hypoxia (Student's t-test, $p < 0.01$).

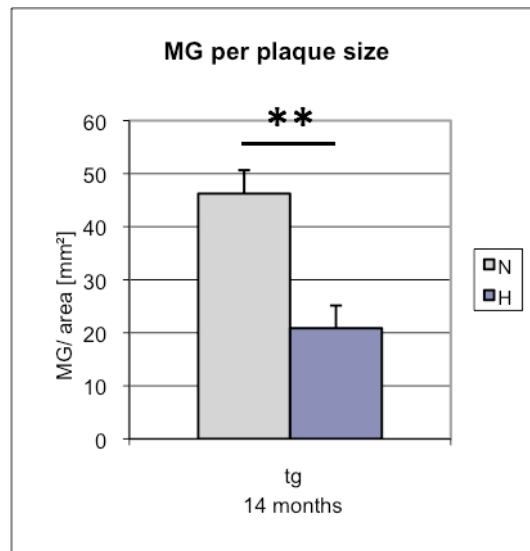


Fig. R17: Plaque occupancy, i.e. number of microglia per mm² of A β - plaque. Plaque occupancy significantly decreases in old, transgenic animals under hypoxia (H, normoxia N) (asterisks indicate a significance of $p < 0.01$, Student's T- test).

Discussion

1. The hypothesis

It is known that increased severity of Alzheimer's disease (AD) is associated with hypoxic conditions of the brain tissue, such as stroke (Schneider et al., 2007; Snowden, 2003). Furthermore, various vascular risk factors are associated with AD (see introduction). Considering this, it was asked whether hypoxia could alter the progression of the disease, in the sense that there is a direct and causal relationship.

We will start by evaluating the model and the methods that were used to answer this question. In the following part, the obtained results will be reflected and discussed in the context of the literature.

2. The model

There are three alternative models to study AD. First, the direct study in humans. This approach delivers the most valid results. However, it is limited. Post-mortem histologic examination of the brain poses no ethical dilemma. But to deliberately cause hypoxic brain conditions in the living subject does, and is not an option.

The second model employs cell cultures. The advantage here lies in the possibility to control many factors of the experiment. But the results are not as valid as in vivo findings. Furthermore, AD poses a complex network of a myriad of partly unknown, interacting factors, such as the behaviour of cell populations. In vitro experiments would not be suitable to study this complexity. It is only after singling out a specific factor to study that cell cultures are an appropriate choice as a model.

The third model to study AD is the use of murine, transgenic animals (Borchelt et al., 1997), as has been done in the present study. However, caution must be taken when translating the results into the human context (and by extension the clinical setting), as it is unlikely to capture its every nuance. The model's advantage is the possibility to expose animals to hypoxic conditions in order to study the effect on AD progression. There are, however, flaws in this model and this particular experimental approach. The murine model of AD only mimics the disease. It sets out from the rather simplistic view that the main pathology in AD is the deposition of A β - plaques. There are two problems with this assumption.

First, the description of the disease is far from complete, with many pathologic processes occurring in parallel and at different times. A complete understanding of the interactions of

these processes is yet not reached. There are certain theories that intend to unify the known facts, such as the amyloid- cascade theory described earlier (see introduction, 1.3.3) (Selkoe, 2002a). But at the time of writing, there is no consensus of what is "the main problem" with AD (Korczyn, 2012). Propositions as to the cause of AD span from accumulation of β -amyloid and subsequent synaptic dysfunction (Selkoe, 2002a), pathogens (Miklossy, 2011), neurovascular pathology (Zlokovic, 2011), convergent pathogenic pathways shared with other neurologic diseases (Ehrnhoefer et al., 2011), mitochondrial dysfunction (Eckert et al., 2011) etc. This is why a model that concentrates on one characteristic is necessarily simplistic and only a variety of models can depict the complexity of the disease (Guerreiro et al., 2011).

The second flaw of the model is this: Human APP and thus human $A\beta$ - protein are expressed in a murine organism. However, it seems that the protein "behaves" similarly as in humans, e.g. aggregating and leading to neurodegeneration. But it is unlikely that the organism's response to the externally inserted protein is the same as in humans. The immune system of humans and mice vary to some degree, and so does a myriad of possible other implicated structures. The interaction between $A\beta$ - protein and the mouse's organism is likely to differ compared to humans.

The experimental approach needs further attention. Hypoxic tissue conditions in the brain were mimicked in a practical but simple manner. This was done by exposing the animals to hypoxia, both terminally (i.e. it lasted until the animals were sacrificed) and continuously, in an especially designed chamber. The animals were not let to adapt to hypoxia in a gradual introduction scheme, instead the stimulus was presented abruptly. The property that was not mimicked closely was the local restriction of hypoxia in brain tissue, as the stimulus was applied to the whole animal. However, it can be theorized that any influence a local hypoxic stimulus might have, a general one would have nonetheless, only more prominently and thus more easily detectable. Furthermore, this approach of general hypoxia has been used by others (Sun et al., 2006; Li et al., 2009).

3. The variables

A large number of variables exists that could potentially be measured to assess the effect of hypoxia on AD. Classically the amount of $A\beta$ - deposition and Tau- tangles are estimated. However, our murine model does not develop the latter. Also the activity, translation and expression of the enzymes and cofactors that jointly manufacture APP into $A\beta$ could be assessed. Apart from this, various cell populations could be examined, e.g. by cell count or assessment of their expressional profiles. This enumeration is only meant to illustrate the

variety of possible approaches and by no means complete. It was decided to concentrate on three variables to measure the effect of hypoxia on AD progression.

First, there is the A β 1-42- protein, known to be the A β - isoform associated with the most detrimental disease progression (Rauk, 2008). Its quantity was determined through histology and ELISA. Secondly, a try was undertaken to estimate its structural quality by assessing the amount of A β - oligomers present. And third, the organism's response to the A β - protein stimulus was investigated with the focus on microglia, in both histology and cell culture.

4. The results

4.1 Hypoxia induces response

First it was demonstrated, that hypoxia induced a systemic response in the animals exposed to it. The hematocrit (HCT), i.e. the percentage of the concentration of red blood cells in blood, is known to increase under hypoxic conditions. As assessed by HCT there was a significant difference between hypoxic animals and those exposed to normoxia. Visually, animals under hypoxia presented with extensive angiogenesis in histology, but this was not quantified. The observed behaviour of the hypoxia group did not differ from controls apart from the fatigue due to this unphysiological stimulus, without observable neurologic deficits. A point of possible critique is that this was not consistently quantified nor recorded. However, the histologic sections were analyzed for strokes or hemorrhagic insults due to increased HCT in the hypoxic animals, but no indication of pathologies could be found.

4.2 Hypoxia and A β - quantity

Hypoxia has been linked to increased levels of A β - protein accumulation (Zhang et al., 2010). Accumulation can be achieved in three different ways: increased production, decreased degradation and slowed down clearance.

This is supported by various findings reported. In post- mortem samples of human AD brains following ischemia, APP levels are elevated (Pluta et al., 1998). As another piece of evidence, it was found that BACE1, the APP cleaving enzyme β - secretase, has a HRE (HIF- responsive element) in its promoter region, and is upregulated under hypoxia in vitro and in vivo in a mouse model (Sun et al., 2006; Zhang et al., 2007). Sun et al. also demonstrated that in a murine mouse model of AD, hypoxia caused an increase in A β 1-42. Another group was able to confirm this (Li et al., 2009). To our knowledge, these groups present the only evidence that A β - protein accumulation increases under hypoxia in vivo.

In the experiments carried out by us, it was not possible to reproduce these findings. Histology and ELISA were employed to determine A β - quantity. None of these methods showed a significant difference in A β - plaque or A β - protein load. This is true for 8 and 14 months old animals.

How can this discrepancy be explained? Although seemingly similar, the approaches pursued by Sun et al. and Li et al. differ from our one in important aspects. All approaches used histology and plaque analysis as well as ELISA to determine A β - protein quantity. But some possible sources of bias can be detected in the two articles cited:

Sun et al. used a different murine AD model, which reduces the comparability to our study. The animals used were 8 months old, which is not a senile age for this species. 8 month- old animals were employed too, but were so as a longitudinal reference point to assess the temporal development of the variables under investigation, e.g. plaque load. However, 14 month- old specimens were also analyzed, an age, that is more representative of senescence in mice. Furthermore, this mimics more closely the conditions found in humans. Sun et al. leave aside this context of old age.

Their counting method for plaques stained in histology is also not beyond criticism: The investigation did not concentrate on one reproducibly identifiable region of the brain for plaque analysis. The hippocampus and its substructure the dentate gyrus were selected, as this has been known as a severely affected structure from AD pathology (Borchelt et al., 1997; Sabuncu et al., 2011; Braak et al., 1993a/b; Schousboe et al., 1993). But besides the advantage of analysing a knowingly affected structure of the brain, it makes it also possible to analyse a higher percentage of that structure. The dentate gyrus was sampled in 5 sections per animal, and 100% of each section was analysed for plaque number and area. Extrapolation from these data is more robust than had one analysed the whole brain at a low sampling rate, e.g. one percent. This is in fact what Sun et al. did. In their approach 10 sections cover the whole brain, without reference to which anatomical structures these sections include and to what degree the respective structures are affected by AD pathology.

Furthermore, their histologic parameter for A β - quantity is plaque number only. Counting plaques by hand is not as reproducible as employing an automated method. No comment is made in the article as to size and staining intensity thresholds, which is important when one wants to determine what to count as a plaque and what not, eventually adding bias. Another point of critique here is that "number of plaques" is alone not a precise measurement for A β - quantity. Hypoxia could hypothetically change the property of the A β - protein, so that it

accumulates in smaller plaques, without any modification of the total A β - quantity. That is why the measurement "plaque area" was employed additionally by us.

Sun et al. used a different method of exposing the animals to hypoxia. The hypoxia group was put into a hypoxic chamber for 16 hours each day, for a total of one month. This procedure is unsuited. For one, it does not mimic the nature of ischemic brain conditions as in stroke, which do not fluctuate in this way. Secondly, a myriad of adaptive mechanisms related to hypoxia is continually "turned on and off", such as stress at exposure. In our model, after a stressful initial period of hypoxic exposure, the animals were left to adapt to this new stimulus. This is also why the validity of the behavioural experiments Sun et al. performed to assess spatial memory deficits employing Morris' water maze can be criticized. They found a significant reduction in spatial memory in the hypoxia group and attribute this to the hypoxic treatment (Sun et al., 2006). As a further point of critique, the normoxia control group was not put in a chamber without the hypoxic stimulus. What this implies is that the behaviour of the hypoxic mice was conditioned towards fear, as they expected suffocation every time they were taken out of the cage. This could possibly alter their behaviour in any behavioural test, without the necessity of there being a structural deficit in the brain. However, the stress which the animals experience in the hypoxia experiments comes mostly from hypoxia itself. "Intrinsic" stress that stems from the respective protocols and procedures, such as conditioned fear, is additional.

The ELISA employed by Sun et al. did not quantify the A β - protein load in the animals, but in cell cultures, making the result not comparable in validity to our ELISA from brain samples.

Li et al. took a similar approach to Sun et al.: The animals' age and the hypoxia exposure procedure were similar to conditions in the experiments of Sun et al.. Their control group has also not been put into the chamber construction, to be exposed there to normoxia. Again, the additional stress associated with the chamber construction and the handling of the animals therein has not been controlled for in both groups, normoxia and hypoxia, but occurred only in the latter. This methodological flaw might affect the experiments' outcome. Furthermore, their quantification procedure for A β - protein from histology is also whole- brain based and methodologically unclear (as concerns sampling areas, thresholds etc.). The ELISA is from brain tissue, but only the "lateral" part of a hemisphere. As discussed earlier, this sampling of the brain for either histology or ELISA without any anatomical basis makes the information obtained less robust. Whole hemispheres were sampled for the ELISA performed.

In summary it can be stated that both articles discussed above show methodological flaws. With a continuous hypoxic exposure, with the control group receiving treatment in the same

chamber and with sampling of defined brain areas, there is no significant difference in the amount of A β 1-42 protein detectable, neither in 8 nor 14 months old animals.

However, there are other findings that have been described *in vitro* and also hint at an A β -protein increase under hypoxia, such as a HIF- binding site in the promoter region of APH-1, a constituent of the γ - secretase cleavage enzyme (Wang et al., 2006). But so far and as to our knowledge, these findings were not reproduced *in vivo*.

4.3 *Hypoxia and A β - quality*

The appearance of A β - protein in the brain stretches from diffuse presence in the monomer form and self- association in oligomers to fibrils that are histologically recognizable as plaques (Rauk, 2008). Influencing the accumulation in a way that hinders plaque formation has been under investigation, but so far it is not clear whether this is beneficial (Hård et al., 2012; Kinghorn et al., 2006). Oligomers have been found to be the most neurotoxic A β -species (Larson et al., 2012).

Initial experiments were carried out to address the hypothesis, that hypoxia leads to an increase in this particular A β - form, i.e. a shift in the spectrum of A β - self accumulation. It was found, that this was indeed the case for a small sample population. But for significant results, future experiments need to investigate this question more deeply. However, this poses an interesting direction of thought: If the overall quantity of A β - protein under hypoxic conditions is not altered, an increase in the oligomer- form could still lead to a more severe and rapid disease progression without affecting the net A β - amount measured. This would have important implications, as there are various attempts to correlate biomarkers, such as A β - and Tau- proteins in the cerebrospinal fluid (CSF) with the disease state, in order to diagnose AD with more precision and predict the disease's progression (Hansson et al., 2006). However, if the oligomer hypothesis is true, these attempts would possibly not be valid.

4.4 *Hypoxia and microglia*

Microglial cells play an important role in inflammation in the brain (Ransohoff et al., 2009). However, no consensus exists as to whether neurodegeneration results from too much or too little inflammation (Lucin et al., 2009), and the effects of inflammation on different cell populations can vary greatly (Covey et al., 2011). In addition, there is no common agreement whether microglial cells are active or reactive players in neuroinflammation, or even victims of it (Graeber et al., 2010). As already described in the introduction, this uncertainty arises from a large variety of microglial phenotypes and subclasses. Some phenotypes are highly

inflammatory and by extension neurotoxic (M1) and some are believed to be neuroprotective (M2), as has been described in detail for macrophages (Mantovani et al., 2004).

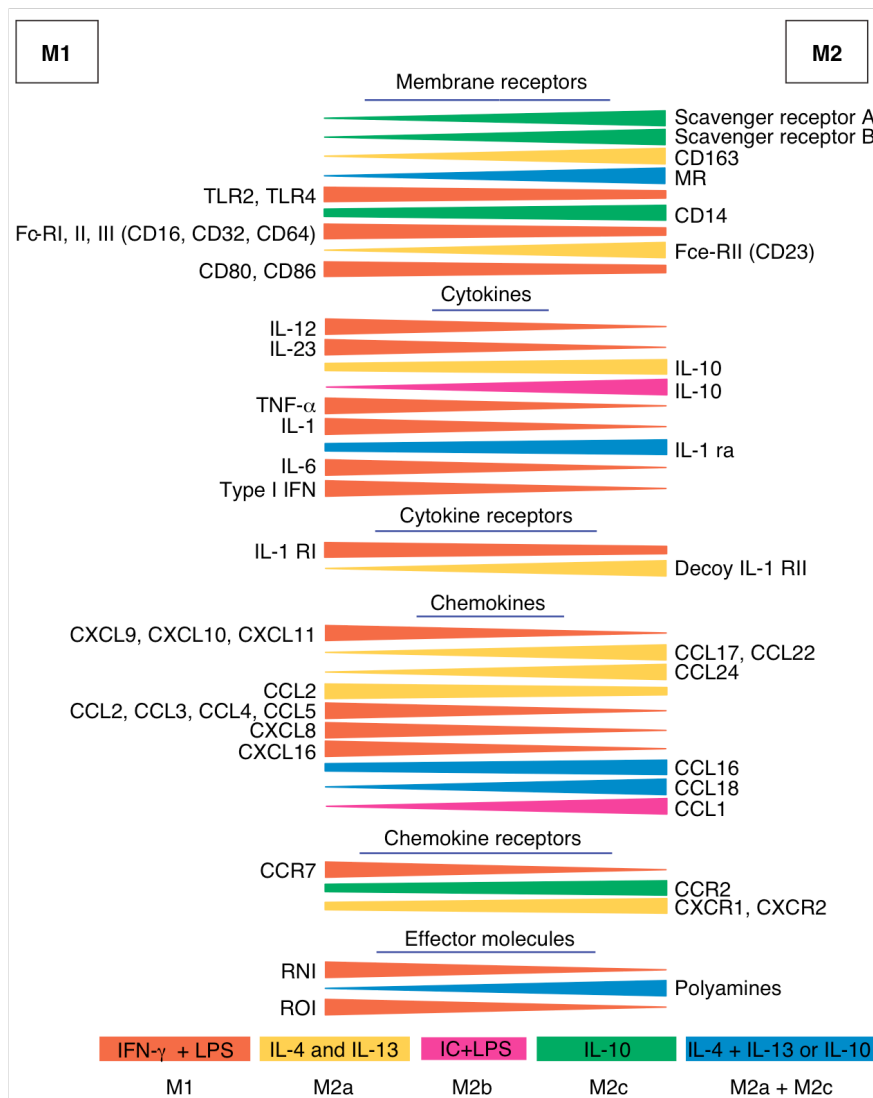


Fig. D01: Illustration of expression profile of M1 and M2 macrophages. Adopted after Mantovani et al. (Mantovani et al., 2004). M1 and M2 activation profiles are presented as extremes of a continuum. A subpopulation of microglia is placed on this continuum depending on its expressional profile, which is a consequence of specific stimuli. See also Fig. D02.

M1 and M2 are the two extremes of a continuum (Fig. D01). A classification within this range is possible according to the expression of selected molecules, i.e. the gene expression pattern determines the polarisation (Mosser, 2003). The respective phenotype of a microglial subpopulation depends on the stimuli presented to it, i.e. its "milieu" (Fig. D02) (Lucin et al., 2009).

For example, A β - proteins have been demonstrated to induce a more neurotoxic phenotype in a microglial population (Jimenez et al., 2008). There are many mechanisms whereby

microglial cells are subsequently able to mediate neuronal death and thus AD progression, e.g. through the expression of iNOS (inducible nitric oxide synthase) (see also Fig. D02, "output") (Brown et al., 2010).

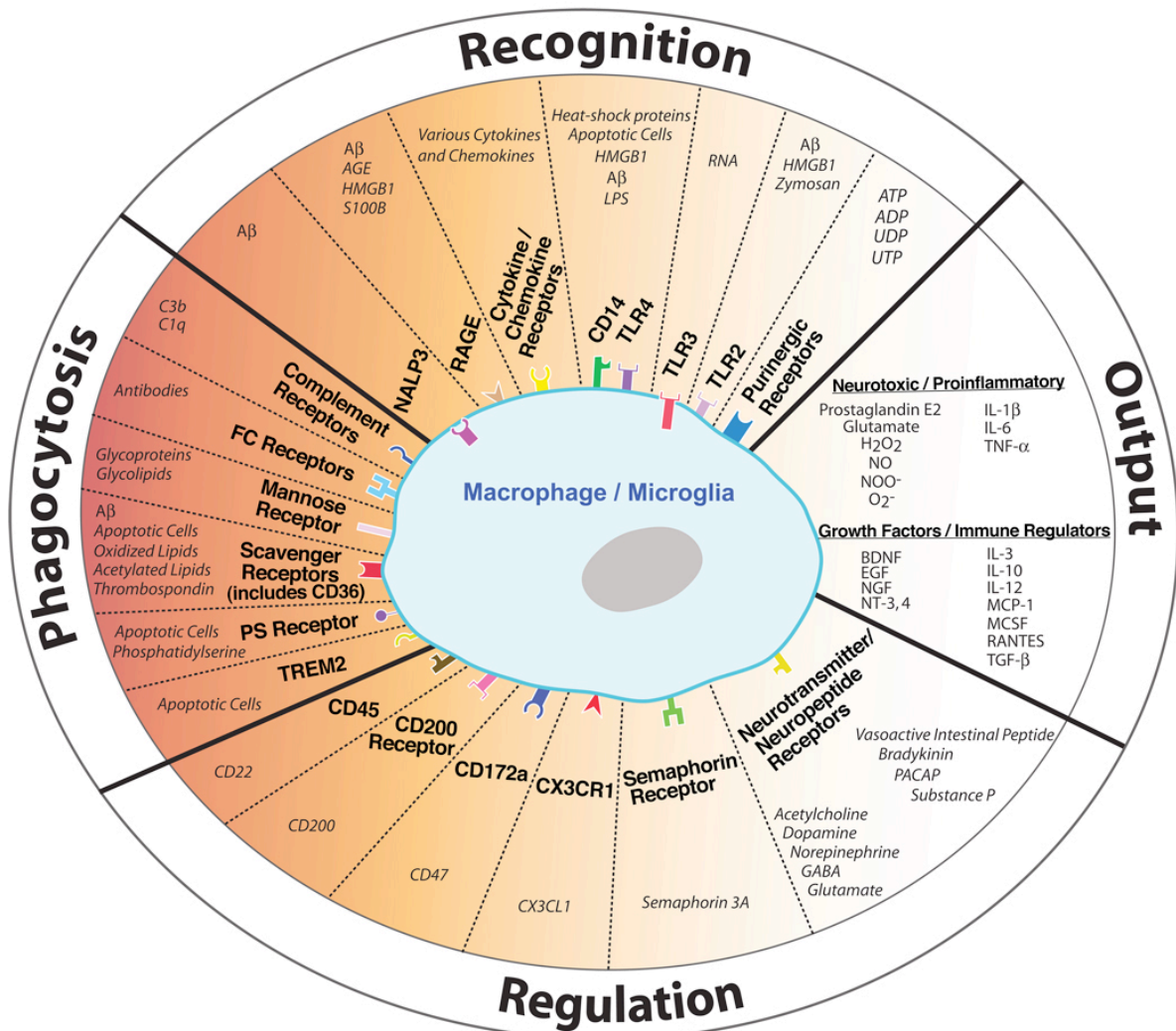


Fig. D02: Diagram of the various characteristics of microglia. Adopted after Lucin & Wyss (Lucin et al. 2009). The various stimuli that can activate microglia into various profiles are depicted under "recognition". "Output" then differs accordingly.

Hypoxia is associated with increased glial activation (Suk et al., 2004). In vitro, glial activation and hypoxia combined induce extensive neurodegeneration, but each condition alone does not (Mander et al., 2005). Glial activation through hypoxia occurs in vivo as well: In humans, PVWD (periventricular white matter damage) is a condition caused by hypoxia of the newborn. The associated neuronal damage is believed to result from hypoxia-mediated activation of microglia. Subsequently, this causes an increased production of inflammatory cytokines, free radicals and NO (Deng et al., 2011). With reference to Fig. D01, the implicated microglial phenotype could be described as M1. An activation of microglia has

further been found to be a key factor for progressive neurodegeneration by mathematical modeling of AD dynamics (Puri et al., 2010).

The number of microglia in the hippocampus was counted as a measure of the quantity of inflammation. In the experiments it was found, that there was an increase in the number of microglia with age and with AD- pathology in the transgenic model. However, the number of microglial cells diminished under long- term exposure to hypoxia.

In old transgenic animals under hypoxia, there was a significant decrease in the number of microglia, when compared to the normoxic control. A decrease in old wild- type animals under hypoxia was found as well, compared to their normoxia controls, although this was not significant. But by changing the statistical test from a multi- group test (ANOVA) to a single- group test (Student's T), the decrease did reach significance. One can hypothesize that with an increase in sample size, significance under the ANOVA- test is possible. To summarize this: Under hypoxia, the number of microglial cells decreases significantly in old transgenic animals as tested by ANOVA.

Microglial cells are known to be involved in A β - protein clearance, for example through phagocytosis (Lee, 2010). A β - plaques attract microglia, which group around a plaque in order to limit its size and degrade it (Fig. MM01, reproduced from the methods & materials section).

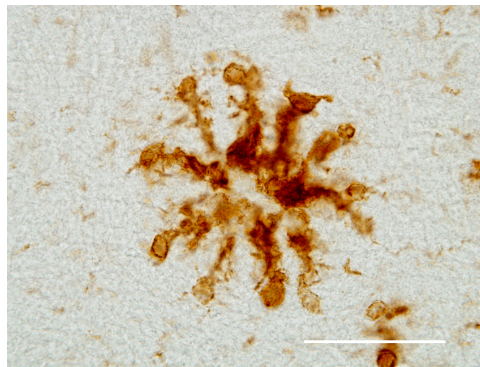


Fig. MM01: Iba1 stained microglia surrounding what appears to be a plaque, scale is 50 μ m

To assesses the microglia function to confront A β - plaques, a metric called "plaque occupancy" was coined. It is defined as the number of microglia in spatial proximity to one square millimeter of A β - plaque. It had been hypothesized that hypoxia would decrease plaque occupancy and it was possible to show, that it did so indeed: The number of microglia roughly halved after long- term exposure to hypoxia, when compared with the normoxia control group.

The decrease in microglia in the experiments has not been described in the literature. However, it is known that microglia respond to short- term hypoxia with activation (Suk, 2004). To test this, murine microglia- enriched cell cultures were prepared (Saura et al., 2003). It was possible to reproduce the finding, that microglial cells respond to a short- term hypoxic stimulus with increased viability as a measure of activation. Despite its limitations in representing the purely microglial reactions to external stimuli as they are in the real brain, namely due to the distortions from signalling of present astrocytes (Saura, 2007), it was decided to use this model, as it is more physiologic than the usage of an immortalized cell culture. A comparable exposure time as in the in vivo model was not feasible due to restricted survival of the cultures. Also, wild- type animals were used for the preparation of the cultures. It can be argued, that the result of increased microglial activity under hypoxia is nevertheless transferable to the AD model: In vivo, a decrease in the number of microglia under long- term hypoxia in wild- type as well as in transgenic animals could be observed. The behaviour of microglia was not qualitatively different in the two groups. It can be inferred that the results from cultured wild- type microglia can be translated equally to the transgenic animals.

To summarize it was found, that microglial cells respond differently to hypoxia in the short- as compared to the long- term. Microglia cells are quite resistant to short hypoxic stimuli. It is known that microglia react to short periods of hypoxia with activation, which it was possible to confirm. However, if the hypoxic exposure is long- term, microglial cells decrease in number, and this correlates positively with vessel density and- it can be argued- oxygen supply. Thus, microglia appear not to be resistant to long- term oxygen deprivation. It can be argued, that microglial behaviour and resistance to hypoxia is a function of the time length of hypoxic exposure, and that it differs greatly between the short and the long run.

4.4.1 A β - quantity is not altered by a decreased number of microglia

Integrating the results so far: Under long- term hypoxia, the A β - quantity does not change (see 4.2 and 4.3), and the number of microglia decreases, compared to the normoxic control. However, one would have suspected the A β - quantity to increase given a decrease in microglia.

This is particularly interesting since microglia are believed to play an important role in clearing A β - protein from the brain (Lee et al., 2010), although the exact mechanism is not known (Hawkes et al., 2012). Various other, non- microglia enzymes have been shown to also degrade A β - proteins (Miners et al., 2011). A β - degradation is thus not entirely dependent on microglia. However, a loss of clearing function might increase the A β - load, and this in turn

would aggravate AD- progression (Lemere et al., 2010), as even small increases in A β - quantity can change the disease's dynamics substantially (Puri et al., 2010). In a murine model of AD, A β - accumulations were almost completely cleared from around the area of induced focal ischemia in the brain, and this was associated with infiltration of microglia (Van Nostrand et al., 2012).

Four explanations are proposed to the phenomenon of unchanged A β - levels despite a decreased number of microglia.

1. First, although microglia internalize the A β - protein formations (Hawkes et al., 2012), it could be that they are not able to degrade them sufficiently (Simard et al., 2006). This has been demonstrated for the oligomer A β - form: microglia do react to A β - protein by activation, but the functions of phagocytosis and clearance are disturbed by it (Pan et al., 2011). It can be argued that clearance takes place but is not effective in degrading A β - protein. Therefore, a decrease in the (deficient) A β - clearance rate through a decrease in the number of microglia would not lead to significant changes in total A β - load. That is, microglial clearance does not "work" to lower the levels of A β - protein, and thus less microglia have no effect on A β - levels.

Interestingly, it has been reported that in murine AD- brains, A β - quantity does not increase overtly despite dysfunctional microglial cells (Mildner et al., 2011). This finding is backed by other groups: Meyer-Luehmann et al. reported that resident microglial cells are not involved in the formation of A β - deposits (Meyer-Luehmann et al., 2008). Grathwohl et al. showed that A β - plaque formation and A β - associated neural damage do not depend on microglial presence, in neither of the two murine models of AD assessed (Grathwohl et al., 2009).

The role microglial cells play in A β - clearance remains disputed. However, the presented findings, from our own laboratory and from the literature, indicate, that this role is minor. Thereby, a decrease in the number of microglia and a subsequent decrease in the microglial clearance rate is likely not to affect the A β - quantity significantly.

2. Second, the remaining microglial cells could compensate functionally for the lost ones, by upregulating proteins that are involved in their clearance function. Such thresholds are known from type- 1 diabetes and familial Parkinson's disease. Accordingly, if the number of functionally valid cells remains above a certain threshold, the function of the cellular population (insulin- producing β - cells of the pancreas and dopaminergic neurons of the substantia nigra, respectively), remains intact. The respective threshold examples are 20%

for type- 1 diabetes (Herold, *Innere Medizin*, 2011) and 30% for Parkinson's disease (Mumenthaler, *Neurologie*, 2008), meaning that this is the minimum amount of cells with which a sufficient function is possible.

There is some evidence that thresholds exist for microglia: Mathematical modelling using data from the literature have yielded microglia density thresholds that are associated with A β -plaque formation (Luca et al., 2003; Quinlan et al., 2005). Surpassing the threshold, microglial density can predict plaque formation. However, due to uncertainty within the parameters of the model, there is a large variation in the microglial density. The variational range of microglial density encompasses levels found in both, AD patients and healthy subjects, limiting the use of the threshold value.

Another study reports, that neurodegeneration occurs once 40% of the microglial population is activated (Rogove et al., 2002). However, caution is advised when interpreting this result. Here, microglia were artificially activated by the injection of the excitotoxin kainate into the murine hippocampus. First, this is not a physiologic stimulus. And second, the resulting activational profile of the microglia (M1) may lack validity.

To summarize, the implication of this hypothesis is that if microglia dropped further in number and below an unknown threshold, which is likely to exist, the resulting loss of the clearance function would lead to detectable increases in the quantity of A β - protein. However, as has been mentioned above, it is questioned whether microglia presence is really necessary for A β - clearance.

3. Clearance of A β - protein from the brain may involve mechanisms, beyond those related to microglia (Lee et al., 2010; Kurz et al., 2011). As the microglial number and the population's function to clear A β - protein drops, compensatory mechanisms may be activated, leading to an unaffected net A β - clearance. One mechanism to achieve this could be the upregulation of the receptor for glycosylated end- products (RAGE) which is located at the blood- brain- barrier (BBB) (Deane et al., 2009). Interestingly, RAGE has recently been shown to be upregulated under hypoxia (Tafani, 2011).

4. Forth, under long- term hypoxia, protein- synthesis of many proteins drops (Semenza, 2011). It could be that the A β - protein synthesis actually drops due to hypoxia, resulting in lower levels of A β - protein. Besides the consideration of the sparse data on this topic (see 4.2), and with the majority being in vitro studies, this hypothesis is not entirely off- ground, especially in the in vivo context. A reduced number of microglia and a subsequently lower

clearance rate would then not result in a detectable net change of A β - load, as the A β - protein synthesis drops also.

4.4.2 *The number of microglia decreases under hypoxia*

Two lines of reasoning are proposed to explain the decrease in the number of microglia under hypoxia.

1. First, in neuronal cultures it has been shown that neither hypoxia nor A β - toxicity affected cell viability to a great extent, but when combined, the two stimuli resulted in significant neuronal degeneration (Mander et al., 2005). It is proposed that microglia behave in a similar fashion. The cell population could be left unaffected by either hypoxia or A β - toxicity alone. But the combination of both could cause the microglia to diminish. As our own experiments in vitro demonstrated and in accordance with what has been demonstrated by others, microglia are activated by hypoxia (Suk et al., 2004). This activation poses a significant challenge to the cell, as many cellular processes are upregulated (Semenza, 2011; Eltzschig et al., 2011). If this activation lasts for a long time due to long- term hypoxia, and if combined with the inherent A β - toxicity of the animal model, the microglial cell population could simply "wear out". The stress imposed could reduce the microglial life- span significantly, resulting in a net loss of microglia. A diminished replenishment and increased vulnerability of microglia with age (Streit, 2006; Graeber et al., 2010) could compromise the microglial tolerance to hypoxia even further. Our observations support this, as the drop in the number of microglia was more severe in old (14 months) than in young (8 months) animals, and slightly more aggravated in transgenic animals than in wild- type controls.

It is also worth considering the length of the microglia- activating stimulus, in our case long- term hypoxia. There is evidence, that long periods of activation, i.e. over- activation, lead to microglial degeneration, with subsequent consequences on brain function (Graeber et al., 2010). The illustration in Fig. D03 comes from the same source. In vitro experiments revealed that over- activation triggers apoptosis (Liu et al., 2001). Another group presented similar results (Polazzi et al., 2006). This is interpreted, in that the microglia cell tries to limit bystander injury to neurons and other structures which would result from excessive activation and proinflammatory factor shedding. Degenerating microglia are also known to be heavily increased in AD (Graeber et al., 2010).

To summarize, there is a distinction to be made between short- and long- term activation of microglia. In the short- term, activated microglia provide support to neurons in distress.

However, long- term activation leads to microglial apoptosis and later neurodegeneration (Fig. D03). In this framework, the different microglial behaviours observed in the experiments (histology and cell culture) can be explained by the different length of the hypoxic stimulus and the subsequent length of microglial activation. In the short- term, microglial cells are activated, but do not diminish. In the long- term, microglial cells undergo apoptosis, which is aggravated by the presence of A β - toxicity.

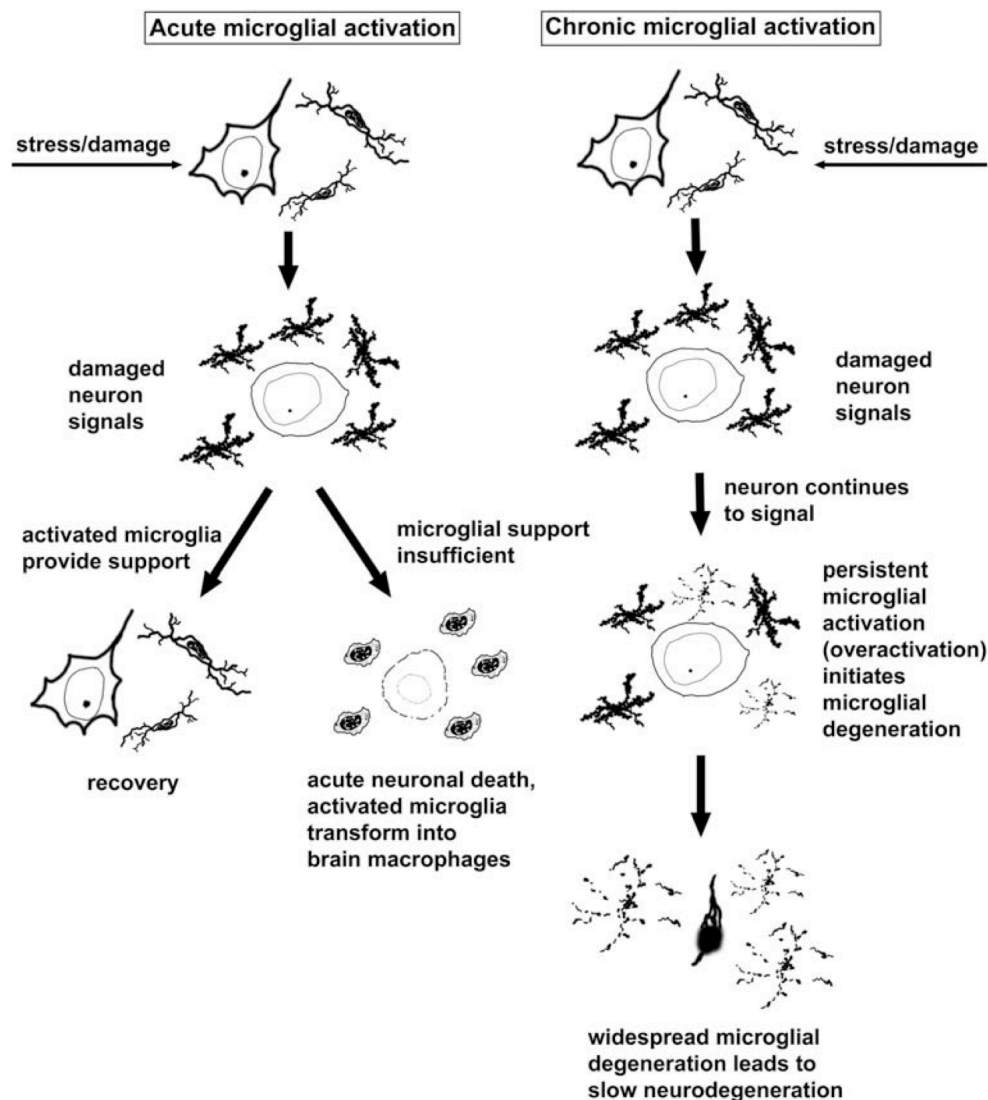


Fig. D03: Illustration of acute and chronic microglial activation, and the different paths this activation leads to. Note that in the case of over- activation, microglia undergo apoptosis potentially to limit collateral damage to neurons and other structures, that are not as easily replaceable. Figure adopted from Graeber et al..

2. Second, the decrease in microglial number could be due to a lower rate of microglial replacement as a consequence of the hypoxic stimulation. As described in the introduction, microglial cells are believed to be a long- lived population of tissue macrophages (Ransohoff et al., 2009). Under inflammatory conditions, peripheral cells can

infiltrate the central nervous system (CNS), and replace or support microglia in their function (Graeber et al., 2010). However, caution is necessary when interpreting these findings: The properties of one species do not translate simply into another one. For example, infiltration of the CNS after peripheral nerve axotomy does occur in mice, but not in rats (Raivich et al., 1998). In humans, migration across the blood brain barrier is a highly complex issue (Larochelle et al., 2011), and differences between rodents and humans are to be expected.

Various studies have been carried out that examined infiltration to the CNS in AD. Khoury et al. found that microglia originate in bone marrow and migrate into the CNS via blood and CCR2, which is a chemokine receptor that mediates migration at the blood brain barrier (El Khoury et al., 2008). Lower migration was associated with higher levels of A β - protein. Another group found immigrating Th2- cells beneficial (Cao et al., 2009). A recent study showed that neither microglia nor bone- marrow derived phagocytes altered AD progression. But restricting CCR2- deficiency to perivascular myeloid cells, another type of macrophage, did affect vascular A β - depositions, but not parenchymal ones (Mildner et al., 2011). This contradicts findings of lower A β - levels after immigration of bone- marrow derived macrophages (Simard et al., 2006). It can be seen that migration of peripheral cells into the CNS is far from understood: It is not agreed upon, to which extent it does take place under physiologic conditions. It is unclear, how translatable results are from one species to another. And the migration that does take place seems to be diverse and its effects will depend on the affected subpopulation of migrating cells, such as microglia or periventricular macrophages. This dynamic is further illustrated by Fig. D04.

It is hypothesized, that the long- term hypoxic stimulus causes a different migration dynamic, possibly through alteration of the blood brain barrier, that could lead to less entry of the brain from the periphery and little replacement of resident microglia. This, together with a higher microglial loss under the stressors at play, could explain the shrinking of the microglia population. Furthermore, the high hematocrit (HCT) as a consequence of the hypoxic treatment changes the physical properties of the blood; it "thickens" so to speak. This could further prevent sufficient migration of cells into the brain.

Summarizing the two possible explanations, the microglia population could have shrunk due to an increased rate of cell death or alternatively due to less replacement, or both combined.

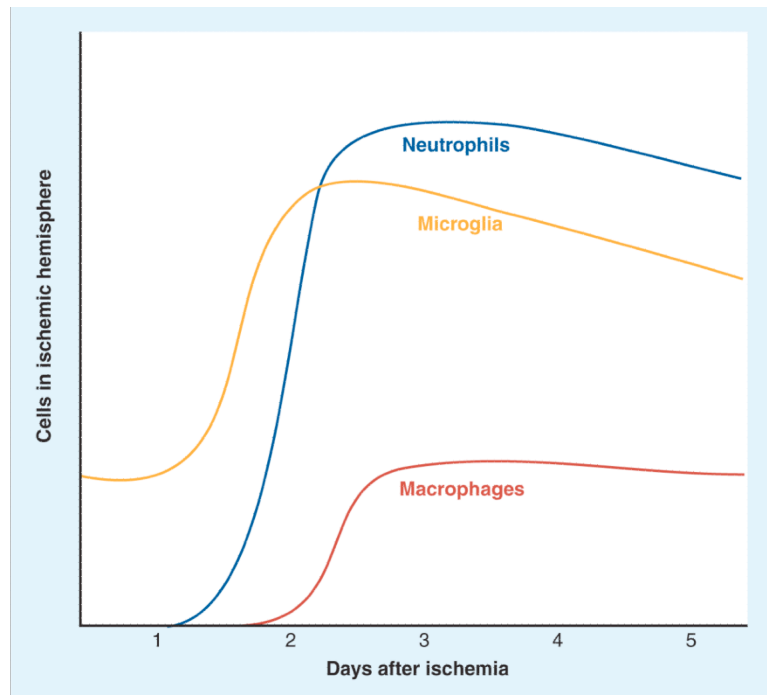


Fig. D04: Dynamics of cellular infiltration of the brain after stroke. Illustration adopted from Weinstein et al.

4.5 Summary

Our results demonstrate that long-term exposure to hypoxia significantly reduces the number of microglia. The reduced number results in significantly reduced plaque occupancy and compromises the function of microglia to confront A β -plaques. The A β 1-42 load, however, is not affected. On the other hand, A β shows an increased trend towards oligomer formation. A variety of possible explanations to these phenomena, that in our opinion deserve further investigation, has been presented.

5. Future research

There are several lines of investigation (A to E) that promise further insight and clarification in the disputed field of AD.

A: Our findings should be supplemented with behavioural tests and the assessment of markers of neuronal damage.

B: Does AD alter, quantitatively or qualitatively, the response to hypoxia, e.g. angiogenesis? The speed and quality of angiogenesis and the regulation of blood homeostasis (e.g. HCT) should be assessed with a longitudinal study with multiple time points of wild-type vs. transgenic animals under hypoxia.

C: Does hypoxia systematically change the A β - protein conformation and accumulation properties? Experiments that measure oligomer quantity according to molecular weight by native Western blotting should be undertaken. Also, the plaque distribution and plaque properties (i.e. diffuse or solid deposition) should be assessed using histology.

D: Further investigation of A β - clearance mechanisms under hypoxia, especially microglia-independent ones, needs to be done. Attention should be focused on the blood- brain barrier and receptors such as RAGE. However, approaches that create a "leaky" blood brain barrier by radiation need to be assessed with caution.

E: The same model should be reproduced with localized tissue hypoxia. This could be achieved through in vivo ligation of specific vessels, i.e. induced strokes, by laser. It would then be possible to clear any disturbing effects that a whole- body scale adaption to hypoxia has on the investigated issue.

Zusammenfassung der Arbeit

Dissertation zur Erlangung des akademischen Grades

Dr. med.

Titel:

Plaque deposition and microglia response under the influence of hypoxia in a murine model of Alzheimer's disease

eingereicht von:

Adrian / Viehweger

angefertigt in / an:

1. Universidad de Sevilla / Instituto de Biomedicina de Sevilla (IBIS) / Hospital Virgen del Rocio / Sevilla
2. Universität Leipzig / Medizinische Fakultät / Universitätsklinikum / Leipzig

betreut von:

1. Prof. J. López Barneo, M.D., Ph.D.
2. A. Pascual Bravo, Ph.D.
3. Prof. Dr. rer. nat. F. Gaunitz
4. Prof. Dr. med. J. Meixensberger

eingereicht im Juni 2012

Clinical findings have linked multiple risk factors and associated pathologies to Alzheimer's disease (AD). Amongst them are vascular risk factors such as hypertension and pathologies such as stroke. Coexistence of AD and these associated pathologies worsenes dementia, the clinical hallmark of the disease, as compared to pure AD. One general common denominator of these associated pathologies is the presence of hypoxic tissue conditions. It was asked the question, whether there exists a mutual, causal interaction between hypoxia and AD pathology, that could explain the clinical observations. Alternatively, the worsened clinical

state of multiple brain pathologies could "simply" be the consequence of multimorbidity, i.e. accumulated disease load, without any causal interaction between the constituents.

To approach this question whether hypoxia influences AD progression, use was made of a murine animal model of AD (transgenic mice: APP^{swe}, PSEN1^{dE}). Animals of two ages (8 and 14 months, "young" and "old" respectively) and two genotypes (transgenic and wild-type) were either treated under hypoxia or normoxia, corresponding to 8% and 21% oxygen, for 20 consecutive days. The resulting changes in the brain were assessed with a variety of techniques, namely by histology, ELISA, dot and Western blotting. Additional experiments in primary cell cultures were performed.

Animals exposed to hypoxia showed an increased hematocrit (HCT), weight loss, reactive angiogenesis, but no infarctions. This illustrates that our hypoxic treatment put significant stress on the animals, without causing major pathologies.

A large number of variables exists that could potentially be measured to assess the effect of hypoxia on AD. The focus was put on three of them: First, there is the A β ₁₋₄₂ protein, known to be the A β - isoform associated with the most detrimental disease progression. In AD, the self-combinatory Amyloid- beta peptide (A β) accumulates in the brain in so-called plaques, which is a main histologic finding of the disease. Its quantity was determined through histology and ELISA.

Secondly, it was attempted to estimate the structural quality of the A β - protein by assessing the amount of A β - oligomers present. A β - protein does self-accumulate in various grades of complexity, i.e. as monomer, oligomer or fibril. Since oligomers are known to be the most neurotoxic "species" of the A β - protein, it was hypothesized that under hypoxic treatment their quantity could increase.

And third, the organism's response to the A β - protein stimulus was investigated. Microglial cells have been described as the first cells to encounter the A β - protein "threat" in the shape of plaques, i.e. A β - protein aggregates. They then try to encapsulate and subsequently degrade them. Therefore, the attention was put on this cellular population.

It was asked whether hypoxia could change the A β - protein quantity in the brain. This was assessed in two ways: First histologically, by staining for A β - protein depositions and quantifying them. Second, an ELISA was performed. Our findings state that hypoxic treatment does not alter the A β ₁₋₄₂ protein load in the brain, neither in young nor old animals, as assessed by histology and by total ELISA quantification of A β ₁₋₄₂ protein.

Since hypoxia did not alter the quantity of the A β - protein, it was asked whether it influenced it qualitatively? If hypoxia increased oligomer formation, this change in the spectrum of the

A β - species could, without any change in total A β - protein load, lead to increased neurotoxicity in animals under hypoxia. Initial experiments showed that oligomer formation in the brain seems to increase. However, this was not statistically significant and future experiments are necessary to evaluate this hypothesis further.

It was then asked, whether hypoxia alters the cellular response to the protein. The total number of microglia in the hippocampal dentate gyrus, our structure of interest for practical purposes, and, it can be argued, by extension the brain, changes dynamically with various factors. First, transgenic animals present an increase in microglia. Second, microglia increase with age. Third, microglia decrease under hypoxia, but only do so significantly in old animals. Next, a parameter called "plaque occupancy" was coined to assess the microglia function to confront A β - plaques. Plaque occupancy is defined as the number of microglia in spatial proximity to one square millimeter of A β - plaque. This means, that microglia restricting one plaque are counted, and then normalized to this plaque's area. It was hypothesized that hypoxia would decrease plaque occupancy. Indeed, plaque occupancy roughly halved under hypoxia.

Summarizing, our results demonstrate that long- term exposure to hypoxia significantly reduces the number of microglia. The reduced number results in significantly reduced plaque occupancy and compromises the function of microglia to confront A β - plaques. The A β 1-42 load, however, is not affected. On the other hand, A β shows an increased trend towards oligomer formation. A variety of possible explanations to these phenomena have been presented, that in our opinion deserve further investigation.

Literature

Aguero-Torres, H., Kivipelto, M. & von Strauss, E. Rethinking the dementia diagnoses in a population-based study: what is Alzheimer's disease and what is vascular dementia?. A study from the kungsholmen project. *Dement Geriatr Cogn Disord* **22**, 244–249 (2006).

Alliot, F., Godin, I. & Pessac, B. Microglia derive from progenitors, originating from the yolk sac, and which proliferate in the brain. *Brain Res. Dev. Brain Res.* **117**, 145–152 (1999).

Alonzo, N. C., Hyman, B. T., Rebeck, G. W. & Greenberg, S. M. Progression of cerebral amyloid angiopathy: accumulation of amyloid-beta40 in affected vessels. *J. Neuropathol. Exp. Neurol.* **57**, 353–359 (1998).

Alzheimer, A. Über eine eigenartige Erkrankung der Hirnrinde. **64**, 146–8 (1907).

Berchtold, N. C. & Cotman, C. W. Evolution in the conceptualization of dementia and Alzheimer's disease: Greco-Roman period to the 1960s. *Neurobiol. Aging* **19**, 173–189 (1998).

Bergem, A. L., Engedal, K. & Kringlen, E. The role of heredity in late-onset Alzheimer disease and vascular dementia. A twin study. *Arch. Gen. Psychiatry* **54**, 264–270 (1997).

Black, S., Gao, F. & Bilbao, J. Understanding white matter disease: imaging-pathological correlations in vascular cognitive impairment. *Stroke* **40**, S48–52 (2009).

Blennow, K., de Leon, M. J. & Zetterberg, H. Alzheimer's disease. *Lancet* **368**, 387–403 (2006).

Borchelt, D. R. *et al.* Accelerated amyloid deposition in the brains of transgenic mice coexpressing mutant presenilin 1 and amyloid precursor proteins. *Neuron* **19**, 939–945 (1997).

Braak, H. & Braak, E. Entorhinal-hippocampal interaction in mnestic disorders. *Hippocampus* **3**, 239–246 (1993a).

Braak, H., Braak, E. & Bohl, J. Staging of Alzheimer-related cortical destruction. *Eur. Neurol.* **33**, 403–408 (1993b).

Breteler, M. M. Vascular risk factors for Alzheimer's disease: an epidemiologic perspective. *Neurobiol. Aging* **21**, 153–160 (2000).

Brown, G. C. & Neher, J. J. Inflammatory neurodegeneration and mechanisms of microglial killing of neurons. *Mol. Neurobiol.* **41**, 242–247 (2010).

Cao, C. *et al.* Abeta-specific Th2 cells provide cognitive and pathological benefits to Alzheimer's mice without infiltrating the CNS. *Neurobiol. Dis.* **34**, 63–70 (2009).

Cheng, I. H. *et al.* Accelerating amyloid-beta fibrillization reduces oligomer levels and functional deficits in Alzheimer disease mouse models. *J. Biol. Chem.* **282**, 23818–23828 (2007).

Chow, V. W., Mattson, M. P., Wong, P. C. & Gleichmann, M. An overview of APP processing enzymes and products. *Neuromolecular Med.* **12**, 1–12 (2010).

Cohen, E., Bieschke, J., Perciavalle, R. M., Kelly, J. W. & Dillin, A. Opposing activities protect against age-onset proteotoxicity. *Science* **313**, 1604–1610 (2006).

Conway, E. M., Collen, D. & Carmeliet, P. Molecular mechanisms of blood vessel growth. *Cardiovasc. Res.* **49**, 507–521 (2001).

Corder, E. H. *et al.* Gene dose of apolipoprotein E type 4 allele and the risk of Alzheimer's disease in late onset families. *Science* **261**, 921–923 (1993).

Covey, M. V., Loporchio, D., Buono, K. D. & Levison, S. W. Opposite effect of inflammation on subventricular zone versus hippocampal precursors in brain injury. *Ann. Neurol.* **70**, 616–626 (2011).

Cummings, B. J., Mason, A. J. L., Kim, R. C., Sheu, P. C.-Y. & Anderson, A. J. Optimization of techniques for the maximal detection and quantification of Alzheimer's-related neuropathology with digital imaging. *Neurobiol. Aging* **23**, 161–170 (2002).

Cummings, J. L. Alzheimer's disease. *N. Engl. J. Med.* **351**, 56–67 (2004).

Dang, C. V. & Semenza, G. L. Oncogenic alterations of metabolism. *Trends Biochem. Sci.* **24**, 68–72 (1999).

de la Torre, J. C. Is Alzheimer's disease a neurodegenerative or a vascular disorder? Data, dogma, and dialectics. *Lancet Neurol* **3**, 184–190 (2004).

de la Torre, J. C. Pathophysiology of neuronal energy crisis in Alzheimer's disease. *Neurodegener Dis* **5**, 126–132 (2008).

Deane, R., Bell, R. D., Sagare, A. & Zlokovic, B. V. Clearance of amyloid-beta peptide across the blood-brain barrier: implication for therapies in Alzheimer's disease. *CNS Neurol Disord Drug Targets* **8**, 16–30 (2009).

Deng, Y. Y., Lu, J., Ling, E.-A. & Kaur, C. Role of microglia in the process of inflammation in the hypoxic developing brain. *Front Biosci (Schol Ed)* **3**, 884–900 (2011).

- Eckert, A., Schmitt, K. & Götz, J. Mitochondrial dysfunction - the beginning of the end in Alzheimer's disease? Separate and synergistic modes of tau and amyloid- β toxicity. *Alzheimers Res Ther* **3**, 15 (2011).
- Ehrnhoefer, D. E., Wong, B. K. Y. & Hayden, M. R. Convergent pathogenic pathways in Alzheimer's and Huntington's diseases: shared targets for drug development. *Nat Rev Drug Discov* **10**, 853–867 (2011).
- El Khoury, J. & Luster, A. D. Mechanisms of microglia accumulation in Alzheimer's disease: therapeutic implications. *Trends Pharmacol. Sci.* **29**, 626–632 (2008).
- Elias, M. F., Wolf, P. A., D'Agostino, R. B., Cobb, J. & White, L. R. Untreated blood pressure level is inversely related to cognitive functioning: the Framingham Study. *Am. J. Epidemiol.* **138**, 353–364 (1993).
- Eltzschig, H. K. & Carmeliet, P. Hypoxia and inflammation. *N. Engl. J. Med.* **364**, 656–665 (2011).
- Farrer, L. A. *et al.* Effects of age, sex, and ethnicity on the association between apolipoprotein E genotype and Alzheimer disease. A meta-analysis. APOE and Alzheimer Disease Meta Analysis Consortium. *JAMA* **278**, 1349–1356 (1997).
- Forette, F. *et al.* Prevention of dementia in randomised double-blind placebo-controlled Systolic Hypertension in Europe (Syst-Eur) trial. *Lancet* **352**, 1347–1351 (1998).
- Garcia-Alloza, M. *et al.* Characterization of amyloid deposition in the APP^{swe}/PS1^{dE9} mouse model of Alzheimer disease. *Neurobiol. Dis.* **24**, 516–524 (2006).
- Giuffrida, M. L. *et al.* The monomer state of beta-amyloid: where the Alzheimer's disease protein meets physiology. *Rev Neurosci* **21**, 83–93 (2010).
- Glenner, G. G. & Wong, C. W. Alzheimer's disease: initial report of the purification and characterization of a novel cerebrovascular amyloid protein. *Biochem. Biophys. Res. Commun.* **120**, 885–890 (1984).
- Goh, K.-I. *et al.* The human disease network. *Proc. Natl. Acad. Sci. U.S.A.* **104**, 8685–8690 (2007).
- Gordon, S. Alternative activation of macrophages. *Nat. Rev. Immunol.* **3**, 23–35 (2003).
- Graeber, M. B. & Streit, W. J. Microglia: biology and pathology. *Acta Neuropathol.* **119**, 89–105 (2010).
- Grathwohl, S. A. *et al.* Formation and maintenance of Alzheimer's disease beta-amyloid plaques in the absence of microglia. *Nat. Neurosci.* **12**, 1361–1363 (2009).
- Guerreiro, R. J. & Hardy, J. Alzheimer's disease genetics: lessons to improve disease modelling. *Biochem. Soc. Trans.* **39**, 910–916 (2011).

Guglielmotto, M. *et al.* The up-regulation of BACE1 mediated by hypoxia and ischemic injury: role of oxidative stress and HIF1alpha. *J. Neurochem.* **108**, 1045–1056 (2009).

Haass, C. *et al.* The Swedish mutation causes early-onset Alzheimer's disease by beta-secretase cleavage within the secretory pathway. *Nat. Med.* **1**, 1291–1296 (1995).

Hansson, O. *et al.* Association between CSF biomarkers and incipient Alzheimer's disease in patients with mild cognitive impairment: a follow-up study. *Lancet Neurol* **5**, 228–234 (2006).

Hård, T. & Lendel, C. Inhibition of Amyloid Formation. *Journal of molecular biology* (2012).doi:10.1016/j.jmb.2011.12.062

Hardy, J. & Selkoe, D. J. The amyloid hypothesis of Alzheimer's disease: progress and problems on the road to therapeutics. *Science* **297**, 353–356 (2002).

Hawkes, C. A., Deng, L., Fenili, D., Nitz, M. & McLaurin, J. In vivo uptake of β -amyloid by non-plaque associated microglia. *Current Alzheimer research* (2012).at <<http://www.ncbi.nlm.nih.gov/pubmed/22272621>>

Heneka, M. T. & O'Banion, M. K. Inflammatory processes in Alzheimer's disease. *J. Neuroimmunol.* **184**, 69–91 (2007).

Iadecola, C. Neurovascular regulation in the normal brain and in Alzheimer's disease. *Nat. Rev. Neurosci.* **5**, 347–360 (2004).

Ivan, C. S. *et al.* Dementia after stroke: the Framingham Study. *Stroke* **35**, 1264–1268 (2004).

Jankowsky, J. L. *et al.* Mutant presenilins specifically elevate the levels of the 42 residue beta-amyloid peptide in vivo: evidence for augmentation of a 42-specific gamma secretase. *Hum. Mol. Genet.* **13**, 159–170 (2004).

Jimenez, S. *et al.* Inflammatory response in the hippocampus of PS1M146L/APP751SL mouse model of Alzheimer's disease: age-dependent switch in the microglial phenotype from alternative to classic. *J. Neurosci.* **28**, 11650–11661 (2008).

Kaelin, W. G., Jr & Ratcliffe, P. J. Oxygen sensing by metazoans: the central role of the HIF hydroxylase pathway. *Mol. Cell* **30**, 393–402 (2008).

Kaur, C. & Ling, E. A. Periventricular white matter damage in the hypoxic neonatal brain: role of microglial cells. *Prog. Neurobiol.* **87**, 264–280 (2009).

- Kawarabayashi, T. *et al.* Age-dependent changes in brain, CSF, and plasma amyloid (beta) protein in the Tg2576 transgenic mouse model of Alzheimer's disease. *J. Neurosci.* **21**, 372–381 (2001).
- Ke, Q. & Costa, M. Hypoxia-inducible factor-1 (HIF-1). *Mol. Pharmacol.* **70**, 1469–1480 (2006).
- Khan, S. & Davies, I. B. Hypoxia and Alzheimer disease. *CMAJ* **178**, 1687; author reply 1687–1688 (2008).
- Kim, S.-H., Tang, Y.-P. & Sisodia, S. S. Abeta star: a light onto synaptic dysfunction? *Nat. Med.* **12**, 760–761; discussion 761 (2006).
- Kinghorn, K. J. *et al.* Neuroserpin binds Abeta and is a neuroprotective component of amyloid plaques in Alzheimer disease. *J. Biol. Chem.* **281**, 29268–29277 (2006).
- Korczyn, A. D. Why have we failed to cure Alzheimer's disease? *J. Alzheimers Dis.* **29**, 275–282 (2012).
- Kurz, A. & Perneczky, R. Amyloid clearance as a treatment target against Alzheimer's disease. *J. Alzheimers Dis.* **24 Suppl 2**, 61–73 (2011).
- Lambert, M. P. *et al.* Diffusible, nonfibrillar ligands derived from Abeta1-42 are potent central nervous system neurotoxins. *Proc. Natl. Acad. Sci. U.S.A.* **95**, 6448–6453 (1998).
- Larochelle, C., Alvarez, J. I. & Prat, A. How do immune cells overcome the blood-brain barrier in multiple sclerosis? *FEBS Lett.* **585**, 3770–3780 (2011).
- Larson, M. E. & Lesné, S. E. Soluble A β oligomer production and toxicity. *J. Neurochem.* **120 Suppl 1**, 125–139 (2012).
- Lee, C. Y. D. & Landreth, G. E. The role of microglia in amyloid clearance from the AD brain. *J Neural Transm* **117**, 949–960 (2010).
- Lemere, C. A. & Masliah, E. Can Alzheimer disease be prevented by amyloid-beta immunotherapy? *Nat Rev Neurol* **6**, 108–119 (2010).
- Lesné, S., Kotilinek, L. & Ashe, K. H. Plaque-bearing mice with reduced levels of oligomeric amyloid-beta assemblies have intact memory function. *Neuroscience* **151**, 745–749 (2008).
- Lesné, S. *et al.* A specific amyloid-beta protein assembly in the brain impairs memory. *Nature* **440**, 352–357 (2006).
- Li, L. *et al.* Hypoxia increases Abeta generation by altering beta- and gamma-cleavage of APP. *Neurobiol. Aging* **30**, 1091–1098 (2009).

- Liu, B. *et al.* Molecular consequences of activated microglia in the brain: overactivation induces apoptosis. *J. Neurochem.* **77**, 182–189 (2001).
- Luca, M., Chavez-Ross, A., Edelstein-Keshet, L. & Mogilner, A. Chemotactic signaling, microglia, and Alzheimer's disease senile plaques: is there a connection? *Bull. Math. Biol.* **65**, 693–730 (2003).
- Lucin, K. M. & Wyss-Coray, T. Immune activation in brain aging and neurodegeneration: too much or too little? *Neuron* **64**, 110–122 (2009).
- Mallard, C., Welin, A.-K., Peebles, D., Hagberg, H. & Kjellmer, I. White matter injury following systemic endotoxemia or asphyxia in the fetal sheep. *Neurochem. Res.* **28**, 215–223 (2003).
- Mander, P., Borutaite, V., Moncada, S. & Brown, G. C. Nitric oxide from inflammatory-activated glia synergizes with hypoxia to induce neuronal death. *J. Neurosci. Res.* **79**, 208–215 (2005).
- Mantovani, A. *et al.* The chemokine system in diverse forms of macrophage activation and polarization. *Trends Immunol.* **25**, 677–686 (2004).
- Mayeux, R. Clinical practice. Early Alzheimer's disease. *N. Engl. J. Med.* **362**, 2194–2201 (2010).
- Meyer, M. R. *et al.* APOE genotype predicts when—not whether—one is predisposed to develop Alzheimer disease. *Nat. Genet.* **19**, 321–322 (1998).
- Meyer-Luehmann, M. *et al.* Rapid appearance and local toxicity of amyloid-beta plaques in a mouse model of Alzheimer's disease. *Nature* **451**, 720–724 (2008).
- Michelucci, A., Heurtaux, T., Grandbarbe, L., Morga, E. & Heuschling, P. Characterization of the microglial phenotype under specific pro-inflammatory and anti-inflammatory conditions: Effects of oligomeric and fibrillar amyloid-beta. *J. Neuroimmunol.* **210**, 3–12 (2009).
- Miklossy, J. Emerging roles of pathogens in Alzheimer disease. *Expert Rev Mol Med* **13**, e30 (2011).
- Mildner, A. *et al.* Distinct and non-redundant roles of microglia and myeloid subsets in mouse models of Alzheimer's disease. *J. Neurosci.* **31**, 11159–11171 (2011).
- Miners, J. S., Barua, N., Kehoe, P. G., Gill, S. & Love, S. A β -degrading enzymes: potential for treatment of Alzheimer disease. *J. Neuropathol. Exp. Neurol.* **70**, 944–959 (2011).
- Morgese, V. J., Elliott, E. J. & Muller, K. J. Microglial movement to sites of nerve lesion in the leech CNS. *Brain Res.* **272**, 166–170 (1983).

- Morimoto, R. I. Stress, aging, and neurodegenerative disease. *N. Engl. J. Med.* **355**, 2254–2255 (2006).
- Mosser, D. M. The many faces of macrophage activation. *J. Leukoc. Biol.* **73**, 209–212 (2003).
- Napoli, I. & Neumann, H. Microglial clearance function in health and disease. *Neuroscience* **158**, 1030–1038 (2009).
- Nimmerjahn, A., Kirchhoff, F. & Helmchen, F. Resting microglial cells are highly dynamic surveillants of brain parenchyma in vivo. *Science* **308**, 1314–1318 (2005).
- Pan, X.-D. *et al.* Microglial phagocytosis induced by fibrillar β -amyloid is attenuated by oligomeric β -amyloid: implications for Alzheimer's disease. *Mol Neurodegener* **6**, 45 (2011).
- Patterson, C. *et al.* Diagnosis and treatment of dementia: 1. Risk assessment and primary prevention of Alzheimer disease. *CMAJ* **178**, 548–556 (2008).
- Perry, V. H., Hume, D. A. & Gordon, S. Immunohistochemical localization of macrophages and microglia in the adult and developing mouse brain. *Neuroscience* **15**, 313–326 (1985).
- Pluta, R., Barcikowska, M., Mossakowski, M. J. & Zelman, I. Cerebral accumulation of beta-amyloid following ischemic brain injury with long-term survival. *Acta Neurochir. Suppl.* **71**, 206–208 (1998).
- Poirier, J. *et al.* Apolipoprotein E polymorphism and Alzheimer's disease. *Lancet* **342**, 697–699 (1993).
- Polazzi, E. & Contestabile, A. Overactivation of LPS-stimulated microglial cells by co-cultured neurons or neuron-conditioned medium. *J. Neuroimmunol.* **172**, 104–111 (2006).
- Puri, I. K. & Li, L. Mathematical modeling for the pathogenesis of Alzheimer's disease. *PLoS ONE* **5**, e15176 (2010).
- Querfurth, H. W. & LaFerla, F. M. Alzheimer's disease. *N. Engl. J. Med.* **362**, 329–344 (2010).
- Quinlan, R. A. & Straughan, B. Decay bounds in a model for aggregation of microglia: application to Alzheimer's disease senile plaques. *Proc. R. Soc. A* **461**, 2887–2897 (2005).
- Raiha, I., Kaprio, J., Koskenvuo, M., Rajala, T. & Sourander, L. Alzheimer's disease in Finnish twins. *Lancet* **347**, 573–578 (1996).

- Raivich, G. *et al.* Immune surveillance in the injured nervous system: T-lymphocytes invade the axotomized mouse facial motor nucleus and aggregate around sites of neuronal degeneration. *J. Neurosci.* **18**, 5804–5816 (1998).
- Ransohoff, R. M. & Perry, V. H. Microglial physiology: unique stimuli, specialized responses. *Annu. Rev. Immunol.* **27**, 119–145 (2009).
- Rauk, A. Why is the amyloid beta peptide of Alzheimer's disease neurotoxic? *Dalton Trans* 1273–1282 (2008).
- Rey, S. & Semenza, G. L. Hypoxia-inducible factor-1-dependent mechanisms of vascularization and vascular remodelling. *Cardiovasc. Res.* **86**, 236–242 (2010).
- Richard, E., Gouw, A. A., Scheltens, P. & van Gool, W. A. Vascular care in patients with Alzheimer disease with cerebrovascular lesions slows progression of white matter lesions on MRI: the evaluation of vascular care in Alzheimer's disease (EVA) study. *Stroke* **41**, 554–556 (2010).
- Rogove, A. D., Lu, W. & Tsirka, S. E. Microglial activation and recruitment, but not proliferation, suffice to mediate neurodegeneration. *Cell Death Differ.* **9**, 801–806 (2002).
- Román, G. C. & Royall, D. R. A diagnostic dilemma: is 'Alzheimer's dementia' Alzheimer's disease, vascular dementia, or both? *Lancet Neurol* **3**, 141 (2004).
- Ruitenbergh, A. *et al.* Cerebral hypoperfusion and clinical onset of dementia: the Rotterdam Study. *Ann. Neurol.* **57**, 789–794 (2005).
- Sabuncu, M. R. *et al.* The dynamics of cortical and hippocampal atrophy in Alzheimer disease. *Arch. Neurol.* **68**, 1040–1048 (2011).
- Saura, J. Microglial cells in astroglial cultures: a cautionary note. *J Neuroinflammation* **4**, 26 (2007).
- Saura, J., Tusell, J. M. & Serratos, J. High-yield isolation of murine microglia by mild trypsinization. *Glia* **44**, 183–189 (2003).
- Savonenko, A. *et al.* Episodic-like memory deficits in the APP^{swe}/PS1^{dE9} mouse model of Alzheimer's disease: relationships to beta-amyloid deposition and neurotransmitter abnormalities. *Neurobiol. Dis.* **18**, 602–617 (2005).
- Schägger, H. Tricine-SDS-PAGE. *Nat Protoc* **1**, 16–22 (2006).
- Schmoltdt, A., Benthe, H. F. & Haberland, G. Digitoxin metabolism by rat liver microsomes. *Biochem. Pharmacol.* **24**, 1639–1641 (1975).

- Schmoltdt, A., Benthe, H. F. & Haberland, G. Digitoxin metabolism by rat liver microsomes. *Biochem. Pharmacol.* **24**, 1639–1641 (1975).
- Schneider, J. A., Arvanitakis, Z., Bang, W. & Bennett, D. A. Mixed brain pathologies account for most dementia cases in community-dwelling older persons. *Neurology* **69**, 2197–2204 (2007).
- Schousboe, A. *et al.* Structural correlates and cellular mechanisms in entorhinal-hippocampal dysfunction. *Hippocampus* **3 Spec No**, 293–301 (1993).
- Scudiero, D. A. *et al.* Evaluation of a soluble tetrazolium/formazan assay for cell growth and drug sensitivity in culture using human and other tumor cell lines. *Cancer Res.* **48**, 4827–4833 (1988).
- Selkoe, D. J. Alzheimer's disease is a synaptic failure. *Science* **298**, 789–791 (2002a).
- Selkoe, D. J. & Podlisny, M. B. Deciphering the genetic basis of Alzheimer's disease. *Annu Rev Genomics Hum Genet* **3**, 67–99 (2002b).
- Semenza, G. L. Targeting HIF-1 for cancer therapy. *Nat. Rev. Cancer* **3**, 721–732 (2003).
- Semenza, G. L. Oxygen sensing, homeostasis, and disease. *N. Engl. J. Med.* **365**, 537–547 (2011).
- Sheng, B. *et al.* Coexisting cerebral infarction in Alzheimer's disease is associated with fast dementia progression: applying the National Institute for Neurological Disorders and Stroke/Association Internationale pour la Recherche et l'Enseignement en Neurosciences Neuroimaging Criteria in Alzheimer's Disease with Concomitant Cerebral Infarction. *J Am Geriatr Soc* **55**, 918–922 (2007).
- Simard, A. R., Soulet, D., Gowing, G., Julien, J.-P. & Rivest, S. Bone marrow-derived microglia play a critical role in restricting senile plaque formation in Alzheimer's disease. *Neuron* **49**, 489–502 (2006).
- Snowdon, D. A. Healthy aging and dementia: findings from the Nun Study. *Ann. Intern. Med.* **139**, 450–454 (2003).
- Sondag, C. M., Dhawan, G. & Combs, C. K. Beta amyloid oligomers and fibrils stimulate differential activation of primary microglia. *J Neuroinflammation* **6**, 1 (2009).
- Soucek, T., Cumming, R., Dargusch, R., Maher, P. & Schubert, D. The regulation of glucose metabolism by HIF-1 mediates a neuroprotective response to amyloid beta peptide. *Neuron* **39**, 43–56 (2003).
- Streit, W. J. Microglial senescence: does the brain's immune system have an expiration date? *Trends Neurosci.* **29**, 506–510 (2006).

Suk, K. Minocycline suppresses hypoxic activation of rodent microglia in culture. *Neurosci. Lett.* **366**, 167–171 (2004).

Sun, X. *et al.* Hypoxia facilitates Alzheimer's disease pathogenesis by up-regulating BACE1 gene expression. *Proc. Natl. Acad. Sci. U.S.A.* **103**, 18727–18732 (2006).

Tafani, M. *et al.* Hypoxia-increased RAGE and P2X7R expression regulates tumor cell invasion through phosphorylation of Erk1/2 and Akt and nuclear translocation of NF- κ B. *Carcinogenesis* **32**, 1167–1175 (2011).

Tjernberg, L. O. *et al.* Controlling amyloid beta-peptide fibril formation with protease-stable ligands. *J. Biol. Chem.* **272**, 12601–12605 (1997).

Van Nostrand, W. E., Davis, J., Previti, M. L. & Xu, F. Clearance of Amyloid- β Protein Deposits in Transgenic Mice following Focal Cerebral Ischemia. *Neurodegener Dis* **10**, 108–111 (2012).

Wang, J.-Y. & Wang, J.-Y. Hypoxia/Reoxygenation induces nitric oxide and TNF-alpha release from cultured microglia but not astrocytes of the rat. *Chin J Physiol* **50**, 127–134 (2007).

Wang, R. *et al.* Transcriptional regulation of A β 1-42 and increased gamma-secretase cleavage of APP and Notch by HIF-1 and hypoxia. *FASEB J.* **20**, 1275–1277 (2006).

Weinstein, J. R., Koerner, I. P. & Möller, T. Microglia in ischemic brain injury. *Future Neurol* **5**, 227–246 (2010).

Weir, E. K., López-Barneo, J., Buckler, K. J. & Archer, S. L. Acute oxygen-sensing mechanisms. *N. Engl. J. Med.* **353**, 2042–2055 (2005).

Wenger, R. H. Cellular adaptation to hypoxia: O₂-sensing protein hydroxylases, hypoxia-inducible transcription factors, and O₂-regulated gene expression. *FASEB J.* **16**, 1151–1162 (2002).

Yan, P. *et al.* Characterizing the appearance and growth of amyloid plaques in APP/PS1 mice. *J. Neurosci.* **29**, 10706–10714 (2009).

Zhang, X. *et al.* Hypoxia-inducible factor 1alpha (HIF-1alpha)-mediated hypoxia increases BACE1 expression and beta-amyloid generation. *J. Biol. Chem.* **282**, 10873–10880 (2007).

Zhang, X. & Le, W. Pathological role of hypoxia in Alzheimer's disease. *Exp. Neurol.* **223**, 299–303 (2010).

Zlokovic, B. V. Neurovascular pathways to neurodegeneration in Alzheimer's disease and other disorders. *Nat. Rev. Neurosci.* **12**, 723–738 (2011).

Erklärung über die eigenständige Abfassung der Arbeit

Hiermit erkläre ich, dass ich die vorliegende Arbeit selbständig und ohne unzulässige Hilfe oder Benutzung anderer als der angegebenen Hilfsmittel angefertigt habe. Ich versichere, dass Dritte von mir weder unmittelbar noch mittelbar geldwerte Leistungen für Arbeiten erhalten haben, die im Zusammenhang mit dem Inhalt der vorgelegten Dissertation stehen, und dass die vorgelegte Arbeit weder im Inland noch im Ausland in gleicher oder ähnlicher Form einer anderen Prüfungsbehörde zum Zweck einer Promotion oder eines anderen Prüfungsverfahrens vorgelegt wurde. Alles aus anderen Quellen und von anderen Personen übernommene Material, das in der Arbeit verwendet wurde oder auf das direkt Bezug genommen wird, wurde als solches kenntlich gemacht. Insbesondere wurden alle Personen genannt, die direkt an der Entstehung der vorliegenden Arbeit beteiligt waren.

.....
Datum

Unterschrift

Curriculum Vitae

Name: Adrian Viehweger

Geboren am 28.10.1986 in Meerane

Schulbildung:

1993 - 1997	Besuch der Grundschule Friedrich Engels in Meerane
1997 - 2002	Besuch des Pestalozzi-Gymnasiums in Meerane
2002	ein Schuljahr übersprungen, Abschluss Klasse 10, Sommerlager in Israel (Vermittlung durch ASF Aktion Sühnezeichen Friedensdienste)
2002 - 2003	Absolvierung eines Schuljahres in Neuseeland, Western Springs College, Auckland
2003 - 2005	Pestalozzi-Gymnasium Meerane, Abitur 07/2005 (1,2)
07/05 - 07/06	Ableistung eines freiwilligen sozialen Jahres in Ecuador als Ersatz für den Zivildienst (gemäß § 14c Abs. 1 des Zivildienstgesetzes der BRD)

Hochschulbildung:

seit 10/06	Medizinstudium an der Universität Leipzig
08/08	Erster Abschnitt der Ärztliche Prüfung/ „Physikum“ (2,0)
03/09 - 03/10	Experimentelle Arbeiten (Neurowissenschaften) im Zuge der Promotion, Instituto de Biomedicina de Sevilla (IBIS), Sevilla, Spanien
seit 10/09	Zweitstudium: Economics and Development (BSc.) an der London School of Economics, International Program (Fernstudium)
seit 04/11	Wissenschaftliche Mitarbeit, Pädiatrische Radiologie, Uniklinik Leipzig, Themenfelder: Evaluation der PET-MRT, DWI und Fetale Hirnentwicklung

Praktika:

02/07 - 03/07	Pflegepraktikum am French Hospital in Jerusalem, Israel
07/07 - 09/07	Pflegepraktikum am Heinrich-Braun-Krankenhaus Zwickau
02/09	Famulatur, Neurochirurgie, Universitätsklinikum Leipzig
09/10	Famulatur, Unfallchirurgie, Heinrich-Braun-Krankenhaus Zwickau
02/11 - 04/11	Forschungspraktikum am Max-Planck-Institut für Kognitions- und Neurowissenschaften
08/11 - 09/11	Praktikum <i>Med- Trainee Programm</i> der HELIOS Kliniken GmbH: Standort: Geschäftsleitung Aue, Projekt: <i>Bedarfsanalyse einer Neurochirurgischen Abteilung am HELIOS Klinikum Aue</i>
09/11- 10/11	Famulatur, Radiologie, Universitätsklinikum Leipzig
03/11	Famulatur, Pathologie, Universitätsklinikum Leipzig

Sprachkenntnisse:

- Englisch, fließend (iBTOEFL 118/120)
- Spanisch, fließend (DELE Nivel Superior, C2)
- Schwedisch (Stufe A2)
- Französisch, Schulkenntnisse

Stipendien:

e- fellows Stipendium seit 2005

Engagement:

2006-08 gewähltes Mitglied im Fachschaftsrat Medizin

Thanks to...

My family and friends for their loving support.

My colleagues at the Institute of Biomedicine, Seville (IBIS), for their patient instruction and generous advice during the course of my research. Special thanks to Alberto Pascual Bravo and Prof. José López Barneo. Not to forget Maria, Lucia, Meriyo, Raquel and Paula.

Prof. Gaunitz and Prof. Meixensberger for their kind advice on the experiments and thorough revision of the manuscript.